

Dear Editor,

Thank you for spending time in handling our manuscript. We also very much thank all of the reviewers for their thoughtful and constructive suggestions and comments that have helped us to improve the quality of the manuscript. Below are our point-by-point responses to each comment, which is in light-blue font color.

Anonymous Referee #1

Jin et al. used an Earth system model with two aerosol schemes that differ in size modes and mixing assumption to study the impact of international shipping emissions (ISE) and natural DMS emissions on cloud radiative effects (CRE) over vast oceanic regions. They found that the regular ISE emissions have a significant global net CRE, which can be further enhanced in a model configuration with reduced DMS emissions. The study also demonstrated that the different aerosol treatments can influence the magnitude and spatial pattern of ISE-induced CRE. The authors suggest a re-evaluation of the ISE-induced CRE with the DMS variability considered. The impact of ISE on CRE is very uncertain. The findings of this study partially explain why the magnitude of ISE-induced CRE has a large spread, shown in the literature. The paper is well written in general and results are clearly presented. However, there are some places in the manuscript that would benefit from further clarification and improvements. I recommend it for publication after the following comments and suggestions are considered.

We appreciate the reviewer's recognition of the potential importance of our manuscript. We carefully revised our manuscript based on the reviewer's comments. The following are our point-by-point responses to these comments.

1) L31-37: Only sulfur emissions are mentioned in the literature review. How about primary particles such as black carbon (BC) and organic carbon (OC)? If both BC and OC from shipping are fixed at the standard emission rate in the various model experiments, please comment on the role of these primary particles, compared to the secondary sulfate converted from sulfur dioxide.

Thanks for raising this important point that we have missed. Yes, both BC and OC from shipping are fixed at the standard emission level in the simulations with shipping emissions turned on. Now we added the following sentence at the end of the second paragraph in the Introduction to address this concern:

“Note that although ISE also contain significant amount of black carbon and organic carbon aerosols, since this study mainly focuses on aerosol induced CRE instead of aerosol direct radiative effect, only primary and secondary sulfate as well as internal mixtures of sulfate and carbonaceous aerosols are addressed due to their much higher hygroscopicity than those of external black carbon and organic carbon aerosols (Pringle et al., 2010),”

2) L74: I don't think the word “diagnose” is properly used here.

We changed “diagnose” to “evaluate”.

3) L78-79: This is inaccurate. Aerosol in CAM5 does not have a direct microphysical influence on convective clouds, but can have an impact indirectly.

We agree with the reviewer and now revised the sentence, as shown here:

“Similar to other climate models, CAM5 does not directly include aerosol’s influence through microphysics on convective clouds, but it allows aerosols to influence convective clouds indirectly, such as by aerosol’s direct effect on circulation, surface evapotranspiration and so on.”

4) L80-96: Are there other differences in aerosol-related treatments between MAM3 and MARC, for example, gas condensation, new particle formation, cloud processing including aqueous-phase chemistry and particle resuspension? What differentiate the BC, OC and sulfate mass for each of the relevant size modes upon emissions? Answers to these questions are critical to understanding the model results in this study (Sect. 3.5), so I suggest including them here.

To address the reviewer’s questions, we added the following paragraph as a new subsection of “2.4 Difference between MARC and MAM3”.

“The most fundamental difference between MARC and MAM is that MARC includes both external and internal mixtures of aerosols in fifteen modes while MAM treats all aerosols as internal mixtures in three modes. As a result, the processes of many aerosol microphysical processes including gaseous condensation, new particle formation, and nucleation scavenging differ between these two models (Kim et al., 2008; Grandey et al., 2018; Rothenberg et al., 2018). “For instance, aerosol activation or nucleation scavenging in MARC and MAM3 is calculated based on competition for water vapor among various types (or modes) of aerosols with different hygroscopicity. In this case, external sulfate modes and the mixture of BC and sulfate (MBS) with BC as core and sulfate as shell would have the same hygroscopicity as sulfate, while external BC and OC would have much lower hygroscopic values. Whereas, MAM calculates this process based on the volume weighted hygroscopicity of each mode based on all the aerosol constitutions within the mode. In that case, the change of individual aerosol species would not influence much the number of activated aerosol substantially” (Rothenberg et al., 2018).”

We have added adequate descriptions of aforementioned differences in the manuscript, or in other cases, direct the reader to corresponding references.

5) L115-116: What is the purpose to treat BC and OC differently in ShipZero and the other three experiments? This is not clearly noted when interpreting the model results (e.g., Figs 4 and 5).

The purpose is to extract the total effects induced by the ISE, i.e., including BC, OC, and sulfur. Figures 4 and 5 are used to address the impacts of various sulfur caps of ISE on CRE. The ISE-induced CRE from various aerosol types is not separated. Only the radiative effects of various aerosol types are diagnosed and presented in Figure 3, such as for BC and OC.

6) L148-150: Are the contributions by aerosol modes or types derived from radiation diagnostics? It is unclear to me whether the radiation diagnostics are done in such a detailed way (by aerosol types). It is counterintuitive to see positive DRE for OC but negative DRE for BC (Figure 3). Any explanations?

Yes, the DRE of each aerosol mode is derived from radiation diagnostics. We double-checked the diagnosed DRE of BC at TOA in all simulations, which are positive at each grid of the globe. Therefore, the negative values of BC DRE in Figure 3 stems from the subtraction (i.e., *ShipRef_DMSRef* minus *ShipZero_DMSRef*). Adding shipping emissions could induce very slight change in the meteorological fields, such as winds, precipitation and so on, which may result in perturbations in the deposition of BC (including both anthropogenic BC over land and shipping BC) and consequently results in negative BC DRE of shipping emissions. It could be the same reason for positive OC DRE induced by shipping emissions.

7) L196-197: Needs clarification on the three numbers. How do they compare to the base case (e.g., *Shipzero_DMSRef*)? It would be interesting to have some discussion about the relative changes in CDNC, compared to the role of sea salt and other types of aerosols.

We calculated the relative changes of column-integrated CDNC induced by shipping emissions by comparing to that in the base case, i.e., *ShipZero_DMSRef*. We revised the corresponding sentence to:

“The increased CWP is closely associated with the increases in the column-integrated CDNC, which changes from $0.305 \times 10^9 \text{ m}^{-2}$ (2.5%, relative to climatological CDNC in *ShipZero_DMSRef* simulation) to $0.476 \times 10^9 \text{ m}^{-2}$ (3.9%) and $0.999 \times 10^9 \text{ m}^{-2}$ (8.3%) on global scale as DMS emission decreases. These results imply that sea salt and DMS emissions are the dominant sources of cloud seeds over remote oceans.”

The contributions to total CDNC from shipping, DMS, sea salt, and transported aerosols from land are an interesting topic and should be qualified in future studies.

8) L200-208: I wonder if clouds in any of these regions are more susceptible to DMS emissions than the others (i.e., relative forcing changes normalized by relative emissions changes).

We appreciate the point from this reviewer, however, we have not collected data with finer temporal resolution in order to carefully calculate this parameter. We have only monthly model output, but it is a good point to check in the future.

9) L220: this sounds like an important claim. The role of any specific type of aerosol in affecting high-latitude clouds depends much on the background total aerosol concentrations. What's the model performance in simulating high-latitude natural and anthropogenic aerosols?

It is hard to evaluate the model performance in simulating high-latitude aerosols, because of a lack of observations (e.g., satellite do not retrieve AOD over very high-latitude regions). By simply comparing high-latitude aerosol loadings in MAM and MARC in another paper of us (<https://doi.org/10.5194/acp-2018-118>), we found that generally, both models simulate very similar magnitude of total AOD in high-latitude; MARC has a slightly lower sea salt and sulfate loadings, a slightly higher BC loading than MAM in high-latitude.

10) L230-242: The two aerosol schemes gave very different results on the magnitude of the ISE-induced CRE, which is my biggest concern. The current explanation is too vague. More in-depth

analysis is required here. Have the two schemes been systematically compared in terms of the global aerosol direct and indirect forcing?

The two aerosols schemes have been systematically compared in another paper (<https://doi.org/10.5194/acp-2018-118>), including aerosol loadings for different aerosol modes, total aerosol optical depth, DRE, CCN, CDNC, and CRE. Differences in some of these variables are obvious. The similar analysis will be performed for shipping emissions. However, current model configuration in this manuscript and the above paper cannot achieve this goal, because some variables such as CCN are not in the model history files in the simulations designed for this manuscript.

To address this concern, we added the following discussion at the end of Section 3.5:
“To track down all the possible reasons for the differences in the ISE-induced CRE between the two aerosol schemes, more detailed analyses on a long chain of processes related to both aerosols and clouds are required, as done by Peters et al. (2014), which is out of the scope of this study and warrants more studies in the future.”

Anonymous Referee #2

This paper addresses the well-known and important topic of negative radiative forcing induced by aerosols formed from international shipping emissions. The paper is novel in addressing natural (DMS) emissions and shipping emissions of aerosols and aerosol precursors simultaneously to study their non-additive contributions to cloud formation and cloud radiative effects (CRE). As an interesting add-on, uncertainties due to microphysics modelling are investigated through the use of different aerosol modules and assumptions on mixing states. The paper is well written and the experiments well designed, properly reflecting the current state of science. I don't have any technical comments beyond those already pointed out by Referee #1.

I recommend publication after the following issues have been addressed:

We thank the reviewer for his/her positive evaluation on our manuscript. We carefully revised the manuscript based on all comments and our point-by-point responses are listed below.

It can be misleading to present the cooling from ISE as balancing GHG warming. E.g. from reading the abstract some may be tempted to conclude that the IMO global sulfur cap from 2020 may contribute to global warming (through reduced CRE), and thus be the wrong way to go. Although global average net radiative forcing may indeed become more positive through this regulation, it should be made clear, at least in the conclusions, that the global sulphur cap is highly beneficial for air quality. The paper already contains relevant references for this (e.g. Corbett et al. 2007, Winebrake et al. 2009). Compensating for GHG warming through aerosol cooling is also problematic because the radiative forcing by aerosols is highly spatially variable. Interestingly in this regard, shipping-induced CRE seems to cause up to 3 W/m² warming (Figure 4) over Central Europe and areas in China and South America. Finally the cooling contribution, as pointed out by this study, has a large uncertainty (while GHG warming is easier to estimate), and the impact on climate parameters (local temperature, precipitation, etc.) from CRE is even more uncertain than the impact on radiative forcing itself.

We appreciate the point of this reviewer and we can understand the concern. In the manuscript, we mainly focus on the ISE-induced negative CRE at TOA averaged over the globe and actually avoid concluding or implying that ISE could induce surface cooling specifically as a balance to GHG warming. On the other hand, we do not believe that it is improper for the reader to conclude from our results that the new IMO sulfur cap from 2020 may partially balance global warming. Additionally, in many places of this manuscript, such as in the first paragraph of Section 4, we did state that reducing the ISE can improve air quality. We also mentioned shipping-induced warming CRE over some regions, such as China and Central Europe. Overall, we believe that we are objective in interpreting our results.

Section 2.4 requires some more text as it is important for correct interpretation of the results. For example, what do you mean by diagnostic and prognostic calls in this context? This may well be obvious to insiders of radiation modelling, but what does it imply for the results presented in this paper? Can effects calculated either in the diagnostic or prognostic calls be compared to each other? Also "In this way, the DRE and CRE of ISE can be isolated and evaluated separately" I don't quite understand this sentence.

The reviewer's point is well taken. We have revised this paragraph by adding more detailed descriptions of calculation steps. Here, by diagnostic we mean the results from radiation calls are not propagated to any actual model physical and dynamical calculations rather than being recorded in output and, therefore, do not influence model integration in the next time step; while by prognostic we mean the results from radiation calls are not only recorded in model history output but also passed to following model calculations and, therefore, affect the results of actual integration.

In our model configuration, the calculations of DRE and CRE of ISE in the diagnostic mode are the same as those in prognostic mode, but diagnostic mode can output the DRE of ISE for each individual aerosol type, such as BC, OC, sulfates, and so on, which are shown in Figure 3.

"In this way, the DRE and CRE of ISE can be isolated and evaluated separately." By this sentence we mean "This is the way we isolate the DRE and CRE of ISE".

The revised paragraph is shown here:

"In the diagnostic mode of CESM-MARC, the DRE are diagnosed by calling the radiation scheme three times in each radiation time step. The first call does not include any aerosols, providing "clean-sky" diagnostics (Ghan, 2013). The second call includes only mineral dust and sea salt aerosols. The third call includes all aerosols. The first and third call are diagnostic, i.e. the radiation budget calculated from these two calls are only used to as model output, therefore they do not influence model integration in the next time step; while the second call is prognostic, i.e., the radiation budget from this call is passed to other model schemes to calculate associated model variables, such as temperature, surface evaporation and so on. Therefore, DRE of only dust and sea salt aerosols are prognostic while all other aerosols including ISE are diagnostic. Note that all radiation variables calculated in these three calls are stored in the model history files for further analyses. In the complimentary MAM3 simulations, the first radiation call (prognostic) includes all aerosols while the second call is a "clean-sky" diagnostic call, excluding all aerosols."

line 50: is from → ranges from

Done.

line 123: Why referring to Corbett et al., 2007 here? The 0.5% cap wasn't mentioned, and plans for 2020 were not known in 2007.

Thanks for pointing this out. Now we removed this citation in the sentence.

line 123: although "International Maritime Organization, 2016" looks like a good reference, in the list of references we only learn "IMO sets 2020 date for ships to with low sulfur fuel oil requirement, 2016" which looks like a log rather than a reference. Is there a link to an accessible report or news release instead?

We apologize for missing the link to this media news. The link to a detailed report on low sulfur fuel oil requirement can be found here:

<http://www.imo.org/en/mediacentre/pressbriefings/pages/mepc-70-2020sulphur.aspx>.

We have also added this link to the references.

line 168: proposed by IMO → decided by IMO

Done.

line 182: demonstrate → exhibit or show

Done.

line 199: illustrate → exhibit or show

Done.

line 201: analysis → analyses

Done.

Short Comment #1

In their study, the authors investigate the uncertainties associated with estimating aerosol indirect effects (AIES) induced by global shipping emissions in a general circulation model. The uncertainties studied here are three-fold, in the sense that 1) AIEs from shipping emissions are shown to non-linearly depend on the background concentration of natural DMS emissions (an expected result and very valuable as it has not been quantified before), 2) AIEs from shipping emissions depend on the amount of sulphur contained in the fuel (as has been shown in earlier studies) and 3) estimated AIEs from shipping emissions depend heavily on the aerosol microphysics module in the general circulation model.

As I have also worked on this topic in the past, I find the study extremely interesting and relevant and I have some comments/remarks concerning the results, the presented analysis and framing of the results presented here in the view of earlier studies.

We truly appreciate Dr. Peters's recognition of the uniqueness of our manuscript and his interest in and comments on our manuscript. We provide our point-by-point response in the following.

Main point: In my view, the discussion of the differences between the two aerosol modules and their impact on the results warrants a bit more investigation/explanation. In Peters et al (2012), P12 in the following, we investigated the uncertainties of AIEs from shipping emissions related to the assumed emission particle size distribution and the total amount of fuel burnt. We found a significant impact of the assumed particle size distribution on the estimated AIEs: assuming all sulphuric compounds being assigned to the soluble Aitken mode at point of emission (as supported by various field observations) leads to significantly more negative AIEs than assigning them half and half to the soluble Accumulation and Coarse modes as was done in the standard AeroCom emission setup (cf P12). This is due to the substantially higher number of primary emitted soluble particles. This was further substantiated in the corrigendum to P12 (Peters et al., 2013), in which a bugfix in the aerosol module lead to an even higher number of emitted particles. My question here is: what size mode are the shipping emissions (and the DMS emissions) assigned to at the point of emission in MAM3 and MARC? This is not described in Section 2, but is a critical point. Compare to the detailed analysis from emission all the way to the resulting effects on cloud properties detailed in Peters et al. (2012, 2014), because in the end, AIEs are the end product of a long chain of processes calculated in various parameterizations with, most certainly, inherent uncertainties. Are there diagnostics of aerosol numbers per mode (see P12) available for the current study so as to investigate the differences between the two aerosol microphysics modules in more detail? This would also help in investigating the interplay with different assumed DMS emission levels, especially for the case of zero DMS emissions where the differences between the two parameterisations are largest. Can CCN diagnostics (see P12, Peters et al. 2014, P14 in the following) be provided to further investigate these points?

We added the following sentences at the end of Section 2.3 to further describe corresponding processes in MARC:

“Note that in MARC model, gas-phase sulfur compounds can be oxidized in both gaseous and aqueous phase to form sulfate that could enter aerosol phase in several pathways: (1) aerosol nucleation to form new nucleation mode sulfate aerosols; (2) condensation of gaseous sulfuric

acid on both external sulfate and carbonaceous aerosols (the latter specifically ages carbonaceous aerosols to form sulfate-carbonaceous aerosol mixtures); and (3) evaporation of cloud and rain drops that resuspends aqueous sulfate to accumulation mode sulfate aerosol (Kim et al., 2008; Grandey et al., 2018; Rothenberg et al., 2018).”

We have compared aerosol loadings of each aerosol type and CCN between MARC and MAM in another paper (Grandey et al., 2018), which is available (<https://doi.org/10.5194/acp-2018-118>).

To address this concern, we added the following discussion at the end of Section 3.5:
“To track down all the possible reasons for the differences in the ISE-induced CRE between the two aerosol schemes, more detailed analyses on a long chain of processes related to both aerosols and clouds are required, as done by Peters et al. (2014), which is out of the scope of this study and warrants more studies in the future. Interesting reader is referred to another paper of ours (Grandey et al., 2018) in addressing this aspect.”

Minor points:

Lines 40-42: please also mention the Corrigendum to P12 – i.e. Peters et al 2013 - as the results from P12 suffered from a bug in the aerosol microphysics module. The results presented in Peters et al (2013) are thus more sound.

Done.

Lines 118 – 126: while investigating the effect of total sulfur content in bunker fuel is an important issue, please also mention uncertainties related to the total amount of fuel burnt (cf P12).

Now we have added the following sentence to address this concern:

“These numbers related to annual sulfur emissions are generally estimated based on the total amount of heavy fuel burnt by ships and the associated emission rates, whose uncertainties were addressed by Peters et al. (2012).”

Lines 170-172: see my above comment regarding an analysis of the causal chain from emissions -> AIEs.

We addressed this causal chain at the end of Section 3.5. Please also see our responses to the “Main point” above.

Lines 178-180: this reads like the increase in CWP leads to an increase in CDNC, but it should be the other way around (at least from the viewpoint of a parameterisation in which a causal connection of cause-and-effect has to be established by design)

In this manuscript, we presented our results in the following order: CRE<-CWP<-CDNC, which tracks back the reason that causes the changes in CRE. We believe that changes in CDNC result in changes in CWP, which in turn causes changes in CRE. Now we revised the sentence to reflect the cause-effect relation:

“The sulfate aerosols from shipping emissions are highly efficient cloud condensation nuclei (CCN) and thus can increase the CDNC, which in turn affects CWP.”

Lines 181-182: this is obvious and is out of place at the end of this paragraph (compare to lines 30-34 in the Introduction)

This sentence is a short and brief summary of Section 3.2 and we revised it to clearly describe the cause-effect relation among ISE emission, CDNC, CWP, and CRE.

Lines 187-192: This is a very interesting paragraph, specifically because DMS emissions are natural and thus an integral part of the climate system and are most probably also included when tuning the TOA radiation balance of the model. Capturing the “correct” background (pre-industrial) aerosol distribution is an extremely difficult task, see e.g. Stevens et al 2017 for the case of developing an aerosol climatology, and is critical for estimating anthropogenic AIEs (as is very nicely shown in this paper). Coming to the point, leaving out DMS emissions results in a quite large TOA radiative imbalance in excess of -5 W m^{-2} (Figure 9). Although the model is constrained by prescribed SSTs, this imbalance, which is much larger on local scales, could have an effect on the results.

We thank the reviewer for raising such an important point. We assume that the reviewer was referring to Figure 6, which shows the ISE-induced CRE with various DMS emissions. When DMS is turned off, the ISE-induced CRE can reach up to 6 W m^{-2} . We agree that this magnitude is very large and warrants further studies. The following sentences are added in this paragraph to emphasize on this point:

“It is worth noting that the ISE-induced CRE can reach up to -6 W m^{-2} when DMS emission is turned off, such as over NPO and NAO, which is a very large negative forcing even on the local scale. Since there are no comparable values in the literature, this large negative forcing warrants a detailed evaluation in future studies using different climate models.”

Lines 266-268: a very important point. Even more importantly, this calls for a reevaluation of aerosol and cloud microphysics parameterisations in general circulation models.

We have revised the sentence to emphasize on the point:

“From the perspective of simulation, this nonlinearity in aerosol activation strongly suggests a reevaluation of CRE induced by shipping and DMS emissions as well as a reevaluation of parameterizations of aerosols–cloud interactions in the general circulation models.”

Lines 269-272: I completely agree. In Peters et al 2011, P11, we applied a specific sampling routine to observational data in order to sample for the effect of shipping emission on cloud properties in “pristine” oceanic areas, where “pristine” was meant with regards to anthropogenic emissions. Looking at the maps displayed in Figure 2, shipping emissions are trumped by DMS emissions in two of the regions sampled in P11: the SE Pacific and the mid-Indian Ocean region. However, the third region investigated in P11, the mid Atlantic, shows a significant contribution of shipping emissions compared to DMS. We also focused more on that region in P14 and

concluded that for “observational studies of AIEs, this highlights the ever so important and often discussed aspect of correctly defining the background (‘pre-industrial’) reference state against which to gauge the present-day observations.” The present study thus very convincingly corroborates our conclusions drawn in 2014.

The importance of correctly defining the background aerosol level has been addressed in many studies, such as P14 mentioned by the reviewer. The uniqueness of conclusions in this manuscript is that the impact of DMS on shipping emission-induced CRE is understudied. Therefore, it has potentially important implication for future studies.

References:

Peters, K., J. Quaas, and H. Graßl (2011), A search for large-scale effects of ship emissions on clouds and radiation in satellite data, *J. Geophys. Res.*, 116, D24205, doi: 10.1029/2011JD016531.

Peters, K., Stier, P., Quaas, J., and Graßl, H.: Aerosol indirect effects from shipping emissions: sensitivity studies with the global aerosol-climate model ECHAM-HAM, *Atmos. Chem. Phys.*, 12, 5985-6007, <https://doi.org/10.5194/acp-12-5985-2012>, 2012

Peters, K., Stier, P., Quaas, J., and Graßl, H.: Corrigendum to "Aerosol indirect effects from shipping emissions: sensitivity studies with the global aerosol-climate model ECHAM-HAM" published in *Atmos. Chem. Phys.*, 12, 5985–6007, 2012, *Atmos. Chem. Phys.*, 13, 6429-6430, <https://doi.org/10.5194/acp-13-6429-2013>, 2013.

Peters, K., Quaas, J., Stier, P. and Graßl, H.: Processes limiting the emergence of detectable aerosol indirect effects on tropical warm clouds in global aerosol-climate model and satellite data, *Tellus B: Chemical and Physical Meteorology*, 66:1, DOI: 10.3402/tellusb.v66.24054, 2014.

Stevens, B., Fiedler, S., Kinne, S., Peters, K., Rast, S., Müsse, J., Smith, S. J., and Mauritsen, T.: MACv2-SP: a parameterization of anthropogenic aerosol optical properties and an associated Twomey effect for use in CMIP6, *Geosci. Model Dev.*, 10, 433-452, <https://doi.org/10.5194/gmd-10-433-2017>, 2017.

We also thank the reviewer for providing these references.

References

Grandey, B. S., Rothenberg, D., Avramov, A., Jin, Q., Lee, H.-H., Liu, X., Lu, Z., Albani, S., and Wang, C.: Effective radiative forcing in the aerosol-climate model CAM5.3-MARC-ARG, *Atmospheric Chemistry and Physics Discussions*, doi:10.5194/acp-2018-118, 2018.

Kim, D., Wang, C., Ekman, A. M. L., Barth, M. C., and Rasch, P. J.: Distribution and direct radiative forcing of carbonaceous and sulfate aerosols in an interactive size-resolving aerosol-climate model, *J Geophys Res-Atmos*, 113, 2008.

Peters, K., Stier, P., Quaas, J., and Grassl, H.: Aerosol indirect effects from shipping emissions: sensitivity studies with the global aerosol-climate model ECHAM-HAM, *Atmos Chem Phys*, 12, 5985-6007, 2012.

- Peters, K., Quaas, J., Stier, P., and Graßl, H.: Processes limiting the emergence of detectable aerosol indirect effects on tropical warm clouds in global aerosol-climate model and satellite data, *Tellus B: Chemical and Physical Meteorology*, 66, 24054, 10.3402/tellusb.v66.24054, 2014.**
- Pringle, K. J., Tost, H., Pozzer, A., Pöschl, U., and Lelieveld, J.: Global distribution of the effective aerosol hygroscopicity parameter for CCN activation, *Atmos Chem Phys*, 10, 5241-5255, 10.5194/acp-10-5241-2010, 2010.**
- Rothenberg, D., Avramov, A., and Wang, C.: On the representation of aerosol activation and its influence on model-derived estimates of the aerosol indirect effect, *Atmos Chem Phys*, 18, 7961-7983, 10.5194/acp-18-7961-2018, 2018.**

1 Impacts on cloud radiative effects induced by coexisting aerosols 2 converted from international shipping and maritime DMS emissions

3 Qinjian Jin¹, Benjamin S. Grandey², Daniel Rothenberg¹, Alexander Avramov^{1†}, Chien Wang^{1,2}

4 ¹Center for Global Change Science, Massachusetts Institute of Technology, Cambridge, Massachusetts, USA.

5 ²Center for Environmental Sensing and Modelling, Singapore–MIT Alliance for Research and Technology, Singapore.

6 † Now at Department of Environmental Science, Emory University, Atlanta, Georgia, USA.

7 *Correspondence to:* Qinjian Jin (jqj@mit.edu)

8 **Abstract.** International shipping emissions (ISE), particularly sulfur dioxide, can influence the global radiation budget by
9 interacting with clouds and radiation after being oxidized into sulfate aerosols. A better understanding of the uncertainties in
10 estimating the cloud radiative ~~effeteffects~~ (CRE) of ISE is of great importance in climate science. Many international shipping
11 tracks cover oceans with substantial natural dimethyl sulfide (DMS) emissions. The interplay between these two major aerosol
12 sources on cloud radiative effects over vast oceanic regions with relatively low aerosol concentration is an intriguing yet poorly
13 addressed issue confounding estimation of the cloud radiative effects of ISE. Using an Earth system model including two aerosol
14 modules with different aerosol mixing configurations, we derive a significant global net CRE of ISE (-0.153 W m^{-2} with ~~$p=0.01$~~
15 ~~and~~ standard error of $\pm 0.004 \text{ W m}^{-2}$) when using emissions consistent with current ship emission regulations. This global net CRE
16 would become much weaker and actually insignificant (-0.001 W m^{-2} ~~with $p=0.98$ and~~ standard error of $\pm 0.007 \text{ W m}^{-2}$) if a more
17 stringent regulation were adopted. We then reveal that the ISE-induced CRE would achieve a significant enhancement when lower
18 DMS emission is prescribed in the simulations, owing to the sub-linear relationship between aerosol concentration and cloud
19 response. In addition, this study also demonstrates that the representation of certain aerosol processes, such as mixing states, can
20 influence the magnitude and pattern of the ISE-induced CRE. These findings suggest a re-evaluation of the ISE-induced CRE with
21 consideration of DMS variability.

22 1 Introduction

23 Marine stratiform clouds have a strong cooling effect on the climate system. They cover about 30% of the global ocean
24 surface (Warren et al., 1988), and can reflect more solar radiation back to space than the dark ocean surface at cloud-free conditions.
25 On the other hand, low-altitude marine stratiform clouds form and develop near to the ocean surface (only several degrees cooler
26 than ocean surface) and thus have limited impacts on the longwave radiation balance (Klein and Hartmann, 1993). Therefore, the
27 annual-mean net radiative effect of cloud at the top of the atmosphere (TOA) is negative (i.e., cooling) and can be up to -20 W
28 m^{-2} on the global scale (Boucher et al., 2013). Consequently, even a few percent change in marine stratocumulus cloud cover can
29 double or offset the anthropogenic global warming due to greenhouse gases.

30 Sulfate aerosols are efficient cloud condensation nuclei and control the formation of marine clouds and their micro- and
31 macro-physical properties (McCoy et al., 2015). The international shipping-emitted sulfur dioxide from combustion of heavy fossil
32 oil (Figure 1) can be oxidized to sulfate aerosols that can increase cloud droplet number concentrations, cloud liquid water path,
33 and planetary albedo, resulting in more solar radiation being reflected back to space, exerting a cooling effect on the climate system
34 (Capaldo et al., 1999; Devasthale et al., 2006; Lauer et al., 2007; Lauer et al., 2009). Although international shipping emissions
35 (ISE) contribute only about 5% ($5.64 \text{ Tg S yr}^{-1}$) to the total anthropogenic sulfur emissions (Corbett and Koehler, 2003; Endresen
36 et al., 2005; Klimont et al., 2013), they dominate the sulfur concentration across much of the ocean, such as the North Pacific

37 Ocean (NPO) and the North Atlantic Ocean (NAO), as shown in Figure 2. Therefore, the radiative impact of the ISE via perturbing
38 marine stratocumulus clouds could be large—especially because marine stratocumulus clouds are often collocated with busy
39 shipping lanes (Neubauer et al., 2014). Note that although ISE also contain significant amount of black carbon and organic carbon
40 aerosols, since this study mainly focuses on aerosol induced CRE instead of aerosol direct radiative effect, we focus on only
41 primary and secondary sulfate aerosols due to their much higher hygroscopicity than those of black carbon and organic carbon
42 aerosols (Pringle et al., 2010).

43 ~~Nevertheless,~~The estimated global annual mean of the ISE-induced net cloud radiative effect (CRE) at TOA has large
44 uncertainties due to the complication in simulating clouds and aerosol–cloud interactions, ranging from -0.60 to -0.07 W m^{-2}
45 (Capaldo et al., 1999; Lauer et al., 2007; Eyring et al., 2010; Righi et al., 2011; Peters et al., 2012; Partanen et al., 2013; Peters et
46 al., 2013). Compared with net CRE, the net direct radiative effect (DRE) of shipping emissions is much weaker, with a magnitude
47 of only -0.08 to -0.01 W m^{-2} , approximately one tenth of the former (Endresen et al., 2003; Schreier et al., 2007; Eyring et al.,
48 2010).

49 Besides shipping-emitted sulfur compounds, oceanic phytoplankton-derived dimethyl sulfide (DMS) is another significant
50 component in the atmospheric sulfur cycle over oceans (Grandey and Wang, 2015; Mahajan et al., 2015; McCoy et al., 2015;
51 Tesdal et al., 2016). DMS can be oxidized by hydroxyl radical or nitrate radical to produce sulfur dioxide and finally converted to
52 sulfate aerosols (Boucher et al., 2003). The global total DMS emission is estimated to range from 8 to 51 Tg S yr^{-1} based on model
53 simulation (Quinn et al., 1993; Dentener et al., 2006); this uncertainty range is itself substantially larger than the total sulfur
54 emissions from shipping. The global annual mean of the DMS-induced net CRE at TOA ~~is~~ ranges from -2.03 to -1.49 W m^{-2}
55 determined by DMS climatology (Gunson et al., 2006; Thomas et al., 2010; Mahajan et al., 2015).

56 Most of the aforementioned studies addressed separately the impacts on CRE of shipping and DMS emissions, largely
57 ignoring the potential nonlinearity in the response of cloud radiative effects to aerosol variations when these sulfate aerosols from
58 two different sources often collocate in the ~~relatively clean~~ marine atmosphere, such as NPO and NAO (Figure 1). The nonlinearity
59 between DMS emission and the associated CRE was studied previously without taking into account the shipping emissions (Pandis
60 et al., 1994; Russell et al., 1994; Gunson et al., 2006; Thomas et al., 2011). Here, to evaluate the CRE induced by both ISE and
61 DMS emissions with a consideration of their interactions, we selected three regions for detailed analysis: the NPO and NAO where
62 the ISE dominate the concentrations of sulfur dioxide and sulfate aerosols, and the Southern Ocean where DMS is the dominant
63 source (Figure 2).

64 This study employs an Earth system model including an interactive aerosol model that simultaneously resolves both
65 external and internal mixtures of sulfate, black carbon, and organic carbon aerosols. Aerosol mixing in this way can resolve aerosol
66 activation process more realistically than either mixing all aerosol species internally or ignoring any mixing at all. By comparing
67 the results with the default aerosol scheme that ~~ignores above~~ assumes internal mixing ~~processes~~, we also quantify the impacts of
68 various assumptions of aerosol mixing states on estimates of the CRE of ISE and DMS emissions. We further quantify the ISE-
69 induced CRE based on various regulations of the International Maritime Organization (IMO) on the fuel sulfur content. Therefore,
70 our findings have important implications for policy makers and future estimates of CRE induced by both ISE and DMS emissions.

71 **2 Methods**

72 **2.1 Climate model**

73 The Community Earth System Model version 1.2.2 (CESM1.2.2) is configured with the Community Atmosphere Model
74 version 5.3 (CAM5.3). CAM5.3 includes a modal aerosol model with an option of 3 or 7 lognormal distributions of aerosol size

75 (MAM3 or MAM7). In this study, a new modal aerosol model—the two-Moment, Multi-Modal, Mixing-state resolving Aerosol
76 model for Research of Climate (MARC; version 1.0.3 here) (Kim et al., 2008; Kim et al., 2014; Rothenberg and Wang, 2016,
77 2017; Grandey et al., 2018) is introduced and used to [diagnose/evaluate](#) both the DRE and CRE of ISE. The details of MARC are
78 described [in the following section below](#). Aerosol DRE are represented by coupling between aerosols and radiation. Aerosol CRE
79 are included by activating aerosols to work as cloud condensation nuclei and ice nuclei in the stratiform clouds (Morrison and
80 Gettelman, 2008; Gettelman et al., 2010). Parameterization of aerosol activation is based on particle size and hygroscopicity of
81 aerosols. Similar to other climate models, CAM5 does not [directly](#) include aerosol’s influence [through microphysics](#) on convective
82 clouds, [but it allows aerosols to influence convective clouds indirectly, such as by aerosol’s effect on circulation, surface](#)
83 [evapotranspiration and so on](#).

84 **2.2 MAM3**

85 The default aerosol scheme in CESM 1.2.2, MAM3, has three modes, each with a lognormal size distribution: Aitken,
86 accumulation, and coarse. Various aerosol species are internally mixed within each mode. Aitken mode is a mixture of sulfate,
87 secondary organic carbon and sea salt; accumulation mode is mixture of sulfate, black carbon, primary organic carbon, secondary
88 organic carbon, dust, and sea salt; coarse mode is a mixture of dust, sea salt, and sulfate (Liu et al., 2012). [MAM3 tracks both the](#)
89 [mass concentration and the number concentration of each aerosol mode](#).

90 **2.3 MARC**

91 MARC uses seven modes with different lognormal size distribution to represent the population of sulfate and
92 carbonaceous aerosols: three modes for [pure](#) sulfate (nucleation or NUC, Aitken or AIT, and accumulation or ACC), one each for
93 pure black carbon (BC) and pure organic carbon (OC), one mixture of BC–sulfate in core-shell structure (MBS), and one mixture
94 of OC–sulfate (internal mixture; MOS). MARC predicts total particle mass and number concentrations while assuming the standard
95 deviation within each of the seven modes to define at any given time the lognormal distribution of particle size. In addition,
96 carbonaceous mass concentrations inside MBS and MOS are also predicted to allow the mass ratios between sulfate and
97 carbonaceous compositions [to](#) evolve over time, changing the optical and chemical properties of the mixed aerosols. The emissions
98 of mineral dust and sea salt that MARC uses are calculated by the land surface model and atmosphere model, respectively
99 (Mahowald et al., 2006; Albani et al., 2014; Scanza et al., 2015). Mineral dust and sea salt are each represented by four bins with
100 fixed sizes in MARC. For details of MARC aerosol mode size distribution and chemical parameters, please refer to [Rothenberg et](#)
101 [al. \(2017\)](#). [Rothenberg and Wang \(2017\)](#). [Note that in MARC model, gas-phase sulfur compounds can be oxidized in both gaseous](#)
102 [and aqueous phase to form sulfate that could enter aerosol phase in several pathways: \(1\) aerosol nucleation to form new nucleation](#)
103 [mode sulfate aerosols; \(2\) condensation of gaseous sulfuric acid on both external sulfate and carbonaceous aerosols \(the latter](#)
104 [specifically ages carbonaceous aerosols to form sulfate-carbonaceous aerosol mixtures\); and \(3\) evaporation of cloud and rain](#)
105 [drops that resuspends aqueous sulfate to accumulation mode sulfate aerosol](#) (Kim et al., 2008; Grandey et al., 2018; Rothenberg et
106 al., 2018).

107 **[2.42.4 Difference between MARC and MAM3](#)**

108 [The most fundamental difference between MARC and MAM is that MARC includes both external and internal mixtures of aerosols](#)
109 [in fifteen modes while MAM treats all aerosols as internal mixtures in three modes. As a result, the processes of many aerosol](#)
110 [microphysical processes including gaseous condensation, new particle formation, and nucleation scavenging differ between these](#)
111 [two models](#) (Kim et al., 2008; Grandey et al., 2018; Rothenberg et al., 2018). [“For instance, aerosol activation or nucleation](#)

112 [scavenging in MARC and MAM3 is calculated based on competition for water vapor among various types \(or modes\) of aerosols](#)
113 [with different hygroscopicity. In this case, external sulfate modes and the mixture of BC and sulfate \(MBS\) with BC as core and](#)
114 [sulfate as shell would have the same hygroscopicity as sulfate, while external BC and OC would have much lower hygroscopic](#)
115 [values. Whereas, MAM calculates this process based on the volume weighted hygroscopicity of each mode based on all the aerosol](#)
116 [constitutions within the mode. In that case, the change of individual aerosol species would not influence much the number of](#)
117 [activated aerosol substantially”](#) (Rothenberg et al., 2018).

118 **2.5 Radiation diagnostics**

119 In the diagnostic mode of CESM-MARC, the DRE are diagnosed by calling the radiation scheme three times in each
120 radiation time step. The first call does not include any aerosols, [providing “clean-sky” diagnostics \(Ghan, 2013\)](#). The second call
121 includes only mineral dust and sea salt aerosols. The third call includes all aerosols. The first and third call are diagnostic ~~while~~
122 ~~the second call is prognostic~~, [i.e. the radiation budget calculated from these two calls are only used to as model output, therefore](#)
123 [they do not influence model integration in the next time step; while the second call is prognostic, i.e., the radiation budget from](#)
124 [this call is passed to other model schemes to calculate associated model variables, such as temperature, surface evaporation and so](#)
125 [on](#). Therefore, DRE of only dust and sea salt aerosols are prognostic while all other aerosols including ISE are diagnostic. [Note](#)
126 [that all radiation variables calculated in these three calls are stored in the model history files for further analyses](#). In the
127 complimentary MAM3 simulations, the first radiation call (prognostic) includes all aerosols while the second call ~~(is a “clean-sky”~~
128 ~~diagnostic)~~ [excludes call, excluding](#) all aerosols.

129 [The DRE of aerosols is calculated by subtracting the TOA radiation in the “clean-sky” call \(no direct aerosol–radiation](#)
130 [interaction\) from that in the call that includes all aerosols. The CRE is calculated by subtracting the TOA radiation at clear-sky](#)
131 [from that at all-sky in the “clean-sky” call \(Ghan, 2013\). The calculation of the DRE and CRE of ISE takes a further step—](#)
132 [subtracting the DRE and CRE in simulation without ISE from that with ISE](#). In this way, the DRE and CRE of ISE can be isolated
133 and evaluated separately. Note that all radiative effects are calculated at TOA.

134 **2.5.6 Experimental design**

135 Three groups of simulations are designed to evaluate: (a) the DRE and CRE of ISE, and (b) the sensitivity of the ISE-
136 induced CRE to both DMS emissions and aerosol mixing assumptions. CAM5 was run at a horizontal resolution of $1.875^\circ \times 2.5^\circ$
137 and 30 vertical layers with sea surface temperature (SST), sea ice, greenhouse gas concentrations prescribed at the level of year
138 2000. The aerosol emissions in year-2000 were used except for modified shipping and DMS emissions. The DMS emission is
139 prescribed with a global annual average of $18.2 \text{ Tg S yr}^{-1}$ in DMS reference simulations (Dentener et al., 2006). Each simulation
140 runs for 32 years driven by 12-month cyclic climatological sea surface temperature, with the first 2 years discarded as spin up.
141 Since the ~~observed SST was used~~ [SSTs were prescribed](#), a 2-year period of spin up should be enough for aerosol concentrations
142 and other model components to reach an equilibrium state (e.g., Righi et al., 2011).

143 The first group uses CESM-MARC and includes four simulations, which share the same DMS reference emissions
144 (*DMSRef*) while differing in four various ISE of sulfur compounds (sulfur dioxide and sulfate) (Table 1). *ShipZero_DMSRef*
145 simulation is integrated excluding all aerosol and aerosol precursor emissions from ISE, i.e., sulfur dioxide, sulfate aerosol, organic
146 carbon aerosol, and black carbon aerosol. The other three simulations—*ShipLow_DMSRef*, *ShipRef_DMSRef*, and
147 *ShipHigh_DMSRef*—include the standard emissions of carbonaceous aerosols (e.g., BC and OC) while use three various emission
148 scenarios of sulfur compounds from ISE. The three emission scenarios are based on the assumptions of sulfur content of the heavy
149 fuel oils for ocean-going ships. Currently, the average sulfur content is 2.7% (Corbett and Koehler, 2003; Endresen et al., 2005),

150 which is equivalent to about 5.64 Tg S year⁻¹, referred to as *ShipRef*. On the other hand, as of 2013 the high sulfur fuel oil that has
151 3.5% sulfur content continued to be permitted outside the Emission Control Areas (Lauer et al., 2009; Winebrake et al., 2009),
152 referred to as *ShipHigh*. However, the IMO has planned to lower the sulfur content to 0.5% outside the Emission Control Areas
153 (Winebrake et al., 2009; Notteboom, 2010; International Maritime Organization, 2016) after 2020, referred to as *ShipLow*. In
154 *ShipLow* and *ShipHigh*, the total global sulfur shipping emissions are 1.0 and 7.2 Tg S year⁻¹, respectively. [These numbers related](#)
155 [to annual sulfur emissions are generally estimated based on the total amount of heavy fuel burnt by ships and the associated](#)
156 [emission rates, whose uncertainties were addressed by](#) Peters et al. (2012). The differences between these three and the zero
157 shipping emission scenarios represent how various regulations on marine fuel influence the ISE-induced CRE.

158 The second group also uses CESM-MARC and is comprised of three pairs of simulations: (*ShipRef_DMSZero*,
159 *ShipZero_DMSZero*), (*ShipRef_DMSLow*, *ShipZero_DMSLow*), and (*ShipRef_DMSRef*, *ShipZero_DMSRef*). [Note that the pair of](#)
160 [\(*ShipRef_DMSRef*, *ShipZero_DMSRef*\) simulations are also part of the first group.](#) The annual emission of DMS is 18.2 Tg S year⁻¹
161 in the *DMSRef* simulations (Dentener et al., 2006; Liu et al., 2012), and half of that in the *DMSLow* simulations. DMS emission is
162 excluded in the *DMSZero* simulations. Each pair of the simulations include *ShipZero* and *ShipRef*, the difference of which
163 represents the ISE-induced impacts. The purposes of the *DMSZero* and *DMSLow* simulations are to quantify the sensitivities of
164 the ISE-induced CRE (i.e., the difference of CRE in each pair of simulations) to DMS emission and the associated large uncertainty
165 in DMS emission, respectively (Quinn et al., 1993; Dentener et al., 2006). DMS emission in the *DMSLow* simulation is 9.1 Tg S
166 year⁻¹, which is close to the lower boundary of DMS emission estimates, i.e., 8 Tg S year⁻¹ (Quinn et al., 1993). Such sensitivities
167 are examined by calculating the differences among the three pairs of DMS simulations.

168 The third group is the same as the second, but using the default MAM3 aerosol module of CAM5.3 in CESM. The purpose
169 for designing the third group is to cross-validate the simulated DMS impacts on the ISE-induced CRE in the second group. One
170 bonus of the third group is to quantify the impacts of using different aerosol modules with different aerosol mixing states on the
171 simulated results. The anthropogenic emissions for [MARC/MAM3, which](#) are [described by Liu et al. \(2012\), differ slightly](#) ~~different~~
172 from those for [MAM3/MARC](#). All of the experiments are summarized in Table 1.

173 3 Results

174 3.1 DRE of ISE

175 The all-sky DRE of various aerosol species from ISE is diagnosed as the difference between *ShipRef_DMSRef* and
176 *ShipZero_DMSRef* and shown in Figure 3. The total ISE can cause a global negative (cooling) DRE of -23.5 mW m⁻², with the
177 strongest negative (cooling) DRE in the areas with intense shipping tracks, such as mid-latitude areas in the Pacific Ocean and
178 Atlantic Ocean, South China Sea, North Indian Ocean, and the Red Sea. The sulfate aerosols in the accumulation mode (i.e., ACC)
179 contribute 89% to the global total DRE, followed by MOS aerosols with a contribution of 22%. Note that OC and MBS has a
180 counteracting warming effect (Remember that all gas-phase and aerosol emissions from shipping have been removed in *ShipZero*
181 scenarios). The contributions of other aerosol species are very limited and their magnitudes are smaller than 6%. The magnitude
182 of the total cooling effect is within the range from -50 to -10 mW m⁻² estimated in previous studies (Endresen et al., 2003;
183 Schreier et al., 2007). The meridional variations of global zonally-averaged total DRE show that the DRE has the strongest cooling
184 effect of -80 mW m⁻² between 30°N and 40°N and becomes weaker towards both polar regions and can be ignored beyond 45°S
185 and 60°N. The all-sky DRE of total aerosols in *ShipLow_DMSRef* and *ShipHigh_DMSRef* have similar patterns to those in
186 *ShipRef_DMSRef* and have magnitudes of +1.0 and -33.0 mW m⁻², respectively. All of the calculated global DRE values except
187 for BC are confident at the 90% level.

188 3.2 CRE of ISE under various shipping emission regulations

189 The CRE of ISE is much stronger than the DRE and shows different spatial patterns under various shipping emission
190 regulations (Figure 4). At the reference level of shipping emissions (*ShipRef_DMSRef*), significant cooling CRE in SW is simulated
191 in areas of intense shipping tracks, such as the mid-latitude Pacific Ocean and the Baffin Bay between Canada and Greenland, with
192 a global average of -0.218 W m^{-2} . The LW CRE shows positive values in some small areas of high latitude, with a global average
193 of $+0.065 \text{ W m}^{-2}$. Consequently, the global net CRE (SW+LW) is -0.153 W m^{-2} with a similar spatial pattern to that of SW. At
194 the high level of shipping emissions (*ShipHigh_DMSRef*), the CRE changes to -0.253 , $+0.073$, -0.179 W m^{-2} for SW, LW, and
195 net, respectively; more areas show significant changes than in *ShipRef_DMSRef*. Note that all of the above values are statistically
196 significant above the 90% confidence level. However, at the low level of shipping emissions (*ShipLow_DMSRef*), fewer areas
197 demonstrate significant changes than in *ShipRef_DMSRef* and *ShipHigh_DMSRef* and the global averages of the CRE are not
198 significant at the 90% confidence level for SW and net. These results indicate that more stringent shipping emission regulation on
199 sulfur content [proposed/decided](#) by the IMO to be applied after 2020 could effectively reduce or even largely eliminate the net CRE
200 induced by ISE.

201 Further analyses demonstrate that the changes in CRE are caused by perturbations in both cloud water path (CWP; Figure
202 S1) and column-integrated cloud droplet number concentrations (CDNC; Figure 5) induced by ISE. Figure S1 demonstrates
203 significant increases in total CWP mainly over the NPO and NAO at the reference and high levels of ISE. The increases in total
204 CWP is largely (87%) attributed to liquid CWP with the remaining contribution (13%) from ice CWP at the reference shipping
205 emission level. Such increases in CWP could reflect more solar radiation to space and thus cause a cooling radiative effect at TOA,
206 as shown in Figure 4. Note that very limited areas in North Pacific Ocean show significant increases in ice CWP, indicating that a
207 small portion of surface shipping emissions could be vertically transported to very high altitude and form ice cloud. At the high
208 level of shipping emissions, a larger increase in CWP is simulated, which is consistent with the cooler radiative effects. However,
209 no significant changes are simulated in total, ice, or liquid CWP at the low level of shipping emissions. Associated with increases
210 in CWP, the column-integrated cloud droplet number concentration (CNDC) also illustrates significant increases at all levels of
211 shipping emission (Figure 5), which collocate with increases in CWP (Figure S1) and decrease in CRE (Figure 4) over the NPO
212 and NAO. The sulfate aerosols from shipping emissions are highly efficient cloud condensation nuclei (CCN) and thus can increase
213 the CDNC-, [which in turn affects CWP](#). Note that cloud area fraction does not [demonstrate/exhibit](#) any significant changes due to
214 shipping emissions (not shown).

215 3.3 CRE of ISE under various DMS emissions

216 The biogenic emissions of DMS over oceans can be oxidized to sulfates and compete against shipping emitted sulfates
217 for CCN and thus could influence the ISE-induced CRE. We find that the shipping emission-induced CRE exhibits significantly
218 different patterns and global averages at different emission levels of DMS (Figure 6). With DMS emissions ranging from the
219 reference level to low and zero levels, the magnitude of the ISE-induced negative CRE at SW increases from 0.218 to 0.457 and
220 2.435 W m^{-2} on global scale, respectively; significant negative CRE is simulated over more areas in the SO. [It is worth noting that](#)
221 [the ISE-induced CRE can reach up to \$-6 \text{ W m}^{-2}\$ when DMS emission is turned off, such as over NPO and NAO, which is a very](#)
222 [large negative forcing even on the local scale. Since there are no comparable values in the literature, this large negative forcing](#)
223 [warrants a detailed evaluation in future studies using different climate models.](#) For CRE at LW, more areas with significant
224 warming are seen in the SO, NPO, and NAO, with the global averages change from $+0.065$ to $+0.073$ and $+0.253 \text{ W m}^{-2}$ when
225 DMS emissions changes from the reference to low and zero levels, respectively. For net CRE, it shares the similar features with
226 those at SW, but with smaller magnitudes.

227 The DMS emissions influence the ISE-induced CRE by perturbing the ISE-induced changes in CWP and column-
228 integrated CDNC (Figures S2 and 7). The shipping emission-induced changes in the total and liquid CWP increase as DMS
229 emission decreases, particularly over the SO, the NPO, and the NAO, while no significant changes are simulated in the ice CWP.
230 The increased CWP is closely associated with the increases in the column-integrated CDNC, which changes from $0.305 \times 10^9 \text{ m}^{-2}$
231 [\(2.5%, relative to climatological CDNC in the *ShipZero* DMSRef simulation\)](#) to $0.476 \times 10^9 \text{ m}^{-2}$ [\(3.9%\)](#) and $0.999 \times 10^9 \text{ m}^{-2}$ [\(8.3%\)](#)
232 on global scale as DMS emission decreases. [These results imply that DMS emissions are the dominant sources of cloud seeds over](#)
233 [remote oceans](#). The most prominent increases in CDNC are seen in the SO, NPO, and NAO. These results suggest important roles
234 of DMS emissions playing in modulating the ISE-induced changes in cloud properties and radiation. Note that cloud area fraction
235 does not ~~illustrate~~[exhibit](#) any significant change (not shown).

236 As demonstrated in the above analysis, the impacts of DMS emissions on cloud response to shipping emissions are the
237 most prominent over the SO, the NPO, and the NAO, so further [analysis](#)[analyses](#) are performed over these three regions. Figure 8
238 shows cloud responses to shipping emission at different DMS emission levels over the three oceanic regions. Generally, cloud
239 responses become weaker and weaker as DMS emission increases from zero (*DMSZero*) to low (*DMSLow*) and reference (*DMSRef*)
240 level over all of the three regions. The most prominent change in cloud response is over the NPO, followed by the NAO and the
241 SO, which is probably due to the higher contribution of shipping emission to the total sulfur dioxide and sulfate aerosols over the
242 NPO than the NAO and the SO (Figure 2b and 2e). The removal of DMS emission (*DMSZero*) has a much stronger influence on
243 cloud response to shipping emission than reducing DMS emission by half (*DMSLow*), indicating a strong non-linear competing
244 effect for CCN between DMS and shipping emission.

245 3.4 CRE of DMS under various shipping emissions

246 Similar to DMS emissions' impacts on the ISE-induced CRE and cloud properties, ISE could also influence the DMS
247 emission-induced CRE and cloud properties. Generally, stronger cooling net CRE (-7.518 vs. -5.611 W m^{-2}) induced by DMS
248 emissions are seen when shipping emissions are ~~ignored~~[absent](#), particularly in areas of intense shipping tracks, such as over the
249 NPO and the NAO (Figure 9). Such a net cooling CRE is mainly the result of SW CRE. Stronger cooling CRE is associated with
250 larger increases in liquid and total CWP (Figure S3) and column-integrated CDNC (Figure S4) in simulations without shipping
251 emissions than those with shipping emissions.

252 It is worth pointing out that DMS emissions have significant warming CRE at LW, particularly over mid- and high-
253 latitude regions in the Southern Hemisphere and high-latitude regions in the Northern Hemisphere regardless of the presence of
254 shipping emissions (Figure 9). Such a warming CRE could be attributed to increases in total cloud area fraction, which is further
255 attributed to increases in the middle and low cloud area fraction in the high-latitude regions in both hemispheres (Figure S5). Our
256 results indicate that DMS is a significant source to CCN in the extremely clean polar regions in both hemispheres.

257 The area-averaged cloud responses over the SO, the NPO, and the NAO, to DMS emissions at different shipping emission
258 levels are shown in Figure 10. Cloud responses to DMS are stronger over the SO than over the NPO and the NAO regardless of
259 the presence of shipping emissions due to the fact that DMS and shipping emissions respectively dominate the sulfur concentrations
260 over the SO, and the NPO and the NAO (Figure 2). Moreover, cloud responses to DMS emissions become much stronger over all
261 of the three oceanic regions when shipping emissions have been removed. However, such changes in cloud responses to DMS due
262 to removal of shipping emissions (i.e., the slopes of the curves) are stronger over the NPO and the NAO than over the SO, which
263 is caused by very limited shipping emissions over the SO. These results again indicate a strong non-linear competing effect for
264 CCN between DMS and shipping emission.

265 3.5 Impacts of choice of aerosol module on the results

266 Besides the impacts of various ISE regulations and DMS emissions on the ISE-induced CRE, various assumptions about
267 the aerosol mixing states could also have an impact. Figure 11 shows the same results as Figure 6 but using [the MAM3 aerosol](#)
268 [module instead of MARC](#). At the reference level of DMS emissions (*DMSRef*), the ISE-induced CRE are generally stronger in
269 MAM3 (SW: -0.319 , LW: $+0.064$, and Net: -0.255 W m^{-2} ; Figure 11) than in MARC [for SW and net radiation](#) (SW: -0.218 , LW:
270 $+0.065$, net: -0.153 W m^{-2} ; Figure 6). More areas with significant cooling CRE are simulated in MAM3 than in MARC,
271 particularly in the Atlantic Ocean, West Pacific Ocean, and North Indian Ocean. At the low level of DMS emissions (*DMSLow*),
272 both the global averages and spatial patterns of the CRE in MAM3 are very similar to those in MARC. The two aerosol modules
273 show the biggest differences in CRE when DMS emissions are excluded (*DMSZero*). MARC simulates strong ISE-induced CRE
274 over tropical regions and the subtropical and mid-latitude areas of the SO, while MAM3 gives no significant CRE over these
275 regions. Generally, the ISE-induced CRE is stronger in MARC than in MAM3 when DMS emissions are excluded. The associated
276 changes in CDNC and CWP due to ISE illustrates similar patterns to changes in CRE (Figures S6 and S7). A possible reason for
277 such differences is the various mixing assumptions about sulfate and sea salt aerosols in MARC (external mixing) versus in MAM3
278 (internal mixing) ~~and warrants further studies~~. [Interested readers are referred to Grandey et al. \(2018\) for discussion of the](#)
279 [differing radiative effects produced by MARC and MAM. To track down all the possible reasons for the differences in the ISE-](#)
280 [induced CRE between the two aerosol schemes, more detailed analyses on a long chain of processes related to both aerosols and](#)
281 [clouds are required, as done by Peters et al. \(2014\), which is out of the scope of this study and warrants more studies in the future.](#)

282 By comparing Figure 8 with Figure 12 we also observe significantly different impacts of DMS emissions on cloud
283 response to shipping emissions (i.e., the slopes of these curves). MAM3 simulates a weaker impact of DMS emissions on cloud
284 response to shipping emissions than MARC, indicating a weaker non-linear competing effect for CCN between DMS and shipping
285 emissions in MAM3 than MARC.

286 4 Conclusions and Discussion

287 Aerosols from ISE could exert significant cooling on the Earth's climate system through aerosol–cloud and aerosol–
288 radiation interactions. To reduce the pollution and climatic effects from this emission source, the IMO set various emission caps
289 on sulfur content of marine fuel oil to be implemented in the future. Using a state-of-the-art climate model, we find that the newly
290 proposed more stringent emission regulations of shipping emissions can effectively reduce the ISE-induced CRE. As demonstrated
291 in our results, reducing sulfur contents from 3.5% to 2.7% and 0.5% could reduce both DRE (from -51.4 to -36.7 and -3.9 mW
292 m^{-2}) and CRE (from -0.179 to -0.153 and -0.001 W m^{-2}) due to ISE, respectively. Although the ISE-induced CRE would be
293 insignificant on a global scale if sulfur contents of ship fuels were reduced to 0.5%, over some regions significant CRE can still be
294 detected—e.g., high latitude regions of the eastern Pacific Ocean. Therefore, implementation of cleaner fuels in shipping sector,
295 such as natural gas, could be a potential solution for completely eliminating sulfate-induced CRE.

296 More importantly, we find that the magnitude and regional spatial pattern of the ISE-induced CRE are highly sensitive to
297 natural DMS emissions. With DMS emissions reducing from 18.2 to 9.1 Tg S yr^{-1} and zero, the ISE-induced net CRE changes
298 from -0.153 to -0.384 and -2.182 W m^{-2} , respectively. On the other hand, the DMS-induced net CRE changes from -5.611 to
299 -7.518 W m^{-2} when shipping emissions at the reference level are removed in the simulations. It is worth noting that DMS is a
300 significant source to CCN in the extremely clean polar regions in both hemispheres. The strong interactions of CRE between DMS
301 and shipping emissions can be attributed to the nonlinearity in the responses of cloud processes to aerosols, particularly the aerosol
302 activation parameterizations (Abdul-Razzak et al., 1998). In a relatively clean environment, activated aerosol number concentration

303 increases as ambient aerosol number concentration increases until reaching a peak at a specific aerosol number concentration, after
304 which it decreases as ambient aerosol number concentration increases unless ambient vapor concentration is drastically increased.
305 In other words, the fraction of activated aerosols decreases as ambient aerosol concentration increases (Figure S8). From the
306 perspective of simulation, this nonlinearity in aerosol activation strongly suggests a reevaluation of CRE induced by shipping and
307 DMS emissions—[as well as a reevaluation of parameterizations of aerosols–cloud interactions in the general circulation models.](#)
308 From the perspective of field measurements of aerosol–cloud relationships, it warrants careful attention when selecting
309 measurement locations—shipping emissions-related measurements should be collected along intense shipping tracks while in areas
310 with as little DMS emissions as possible to avoid contamination from DMS, and vice versa. Moreover, locations containing both
311 shipping and DMS emissions should also be identified and sampled, in order to investigate non-linear interactions between the
312 emissions.

313 Finally, we find that two different aerosol schemes, with different representations of aerosol mixing state, could produce
314 a large difference (about 67%) in the ISE-induced global CRE. Generally, MARC aerosol module shows stronger nonlinear cloud
315 response to DMS and shipping emissions than MAM3. Overall, numerical studies on the uncertainties in the shipping emission-
316 induced CRE due to various ISE regulations, aerosol interactions, and aerosol mixing states can provide useful information for
317 policy makers and have implications for future projections of anthropogenic climate change.

318 Besides the above-mentioned contributors to the uncertainty in estimating the CRE induced by shipping emissions, spatial
319 resolution of the model is another significant source of this uncertainty. Possner et al. (2016) found that the ship-induced shortwave
320 CRE could increase by a factor of two as model spatial resolution decreases from 1 km to 50 km. With higher spatial resolution,
321 models can resolve fine-scale dynamical processes and feedbacks, such as interaction between aerosol and cumulus clouds
322 (Malavelle et al., 2017). Though model resolution-induced uncertainty is not the focus of this study, it should be taken into account
323 when interpreting the spread of shipping-induced CRE in studies of multi-model comparison.

324 Though we employed a state-of-the-art climate model in this study, it is not without caveats, given that neither MARC
325 nor MAM (including both MAM3 and MAM7 in CAM5) aerosol modules treat nitrate aerosols because of the high computational
326 expense for related aerosol-gaseous chemistry and aerosol thermodynamics calculations (Liu et al., 2012). Lack of treating nitrate
327 aerosols could result in uncertainties in our results based on the fact that both mass of nitrate aerosols emitted from international
328 shipping (e.g., Righi et al., 2011) and their hygroscopicity values (e.g., Kawecki and Steiner, 2018) are very similar to those of
329 sulfate aerosols, and thus nitrate aerosols could have non-negligible competing effects on CRE with sulfate aerosols. Despite that
330 some of the results from this study could be used to qualitatively project the potential outcome, a quantitative assessment should
331 be facilitated to address this topic with an improved model.

332 **Acknowledgments**

333 This study is supported by Concawe, whose mission is to conduct research on environmental issues relevant to the oil refining
334 industry. This research is also partially supported by the U.S. National Science Foundation (AGS-1339264), the U.S. Department
335 of Energy (DE-FG02-94ER61937), and the National Research Foundation (NRF) of Singapore under its Campus for Research
336 Excellence and Technological Enterprise programme. The Center for Environmental Sensing and Modeling (CENSAM) is an
337 interdisciplinary research group of the Singapore-MIT Alliance for Research and Technology (SMART). The CESM project is
338 supported by the National Science Foundation and the Office of Science (BER) of the U.S. Department of Energy. We would like
339 to acknowledge high-performance computing support from Yellowstone (ark:/85065/d7wd3xhc) provided by NCAR's
340 Computational and Information Systems Laboratory, sponsored by the National Science Foundation.

341 **Conflict of interest**

342 The authors declare no competing interests.

343 **Data and code availability**

344 The MARC source code is available via https://github.mit.edu/marc/marc_cesm/ and also archived with DOI
345 10.5281/zenodo.1117370, along with documentation on how to install and run the model. The commit 23e08fe was used in this
346 study. All the analysis code and model output data analyzed are available via
347 <https://drive.google.com/drive/folders/1GHjrpvO06mzC8iFyT0Eif0PRiI56cReV?usp=sharing>.

348

349

References

350

351 Abdul-Razzak, H., Ghan, S. J., and Rivera-Carpio, C.: A parameterization of aerosol activation - 1. Single aerosol type, *J Geophys Res-Atmos*,
352 103, 6123-6131, 1998.

353 Albani, S., Mahowald, N. M., Perry, A. T., Scanza, R. A., Zender, C. S., Heavens, N. G., Maggi, V., Kok, J. F., and Otto-Bliesner, B. L.:
354 Improved dust representation in the Community Atmosphere Model, *J Adv Model Earth Sy*, 6, 541-570, 2014.

355 Boucher, O., Moulin, C., Belviso, S., Aumont, O., Bopp, L., Cosme, E., von Kuhlmann, R., Lawrence, M. G., Pham, M., Reddy, M. S., Sciare,
356 J., and Venkataraman, C.: DMS atmospheric concentrations and sulphate aerosol indirect radiative forcing: a sensitivity study to the
357 DMS source representation and oxidation, *Atmos Chem Phys*, 3, 49-65, 2003.

358 Boucher, O., Randall, D., Artaxo, P., Bretherton, C., Feingold, G., Forster, P., Kerminen, V.-M., Kondo, Y., Liao, H., Lohmann, U., Rasch, P.,
359 Satheesh, S. K., Sherwood, S., Stevens, B., and Zhang, X. Y.: Clouds and Aerosols, in: *Climate Change 2013: The Physical Science
360 Basis. Contribution of Working Group I to the Fifth Assessment Report of the Intergovernmental Panel on Climate Change*, edited
361 by: Stocker, T. F., Qin, D., Plattner, G.-K., Tignor, M., Allen, S. K., Boschung, J., Nauels, A., Xia, Y., Bex, V., and Midgley, P. M.,
362 Cambridge University Press, Cambridge, United Kingdom and New York, NY, USA, 571–658, 2013.

363 Capaldo, K., Corbett, J. J., Kasibhatla, P., Fischbeck, P., and Pandis, S. N.: Effects of ship emissions on sulphur cycling and radiative climate
364 forcing over the ocean, *Nature*, 400, 743-746, 1999.

365 Corbett, J. J., and Koehler, H. W.: Updated emissions from ocean shipping, *J Geophys Res-Atmos*, 108, 2003.

366 Dentener, F., Kinne, S., Bond, T., Boucher, O., Cofala, J., Generoso, S., Ginoux, P., Gong, S., Hoelzemann, J. J., Ito, A., Marelli, L., Penner, J.
367 E., Putaud, J. P., Textor, C., Schulz, M., van der Werf, G. R., and Wilson, J.: Emissions of primary aerosol and precursor gases in the
368 years 2000 and 1750 prescribed data-sets for AeroCom, *Atmos Chem Phys*, 6, 4321-4344, 2006.

369 Devasthale, A., Kruger, O., and Grassl, H.: Impact of ship emissions on cloud properties over coastal areas, *Geophys Res Lett*, 33, 2006.

370 Endresen, O., Sorgard, E., Sundet, J. K., Dalsoren, S. B., Isaksen, I. S. A., Berglen, T. F., and Gravir, G.: Emission from international sea
371 transportation and environmental impact, *J Geophys Res-Atmos*, 108, 2003.

372 Endresen, O., Bakke, J., Sorgard, E., Berglen, T. F., and Holmvang, P.: Improved modelling of ship SO₂ emissions - a fuel-based approach,
373 *Atmos Environ*, 39, 3621-3628, 2005.

374 Eyring, V., Isaksen, I. S. A., Berntsen, T., Collins, W. J., Corbett, J. J., Endresen, O., Grainger, R. G., Moldanova, J., Schlager, H., and
375 Stevenson, D. S.: Transport impacts on atmosphere and climate: Shipping, *Atmos Environ*, 44, 4735-4771, 2010.

376 Gettelman, A., Liu, X., Ghan, S. J., Morrison, H., Park, S., Conley, A. J., Klein, S. A., Boyle, J., Mitchell, D. L., and Li, J. L. F.: Global
377 simulations of ice nucleation and ice supersaturation with an improved cloud scheme in the Community Atmosphere Model, *J
378 Geophys Res-Atmos*, 115, 2010.

379 Grandey, B. S., and Wang, C.: Enhanced marine sulphur emissions offset global warming and impact rainfall, *Scientific Reports*, 5, 2015.

380 Grandey, B. S., Rothenberg, D., Avramov, A., Jin, Q., Lee, H.-H., Liu, X., Lu, Z., Albani, S., and Wang, C.: Effective radiative forcing in the
381 aerosol-climate model CAM5.3-MARC-ARG, *Atmospheric Chemistry and Physics Discussions*, 1-39, 10.5194/acp-2018-118, 2018.

382 Gunson, J. R., Spall, S. A., Anderson, T. R., Jones, A., Totterdell, I. J., and Woodage, M. J.: Climate sensitivity to ocean dimethylsulphide
383 emissions, *Geophys Res Lett*, 33, 2006.

384 International Maritime Organization: IMO sets 2020 date for ships to comply with low sulphur fuel oil requirement,

385 <http://www.imo.org/en/MediaCentre/PressBriefings/Pages/MEPC-70-2020sulphur.aspx>, 2016.

386 Kawecki, S., and Steiner, A. L.: The Influence of Aerosol Hygroscopicity on Precipitation Intensity During a Mesoscale Convective Event, *J
387 Geophys Res-Atmos*, 123, 424-442, 2018.

388 Kim, D., Wang, C., Ekman, A. M. L., Barth, M. C., and Rasch, P. J.: Distribution and direct radiative forcing of carbonaceous and sulfate
389 aerosols in an interactive size-resolving aerosol-climate model, *J Geophys Res-Atmos*, 113, 2008.

390 Kim, D., Wang, C., Ekman, A. M. L., Barth, M. C., and Lee, D. I.: The responses of cloudiness to the direct radiative effect of sulfate and
391 carbonaceous aerosols, *J Geophys Res-Atmos*, 119, 1172-1185, 2014.

392 Klein, S. A., and Hartmann, D. L.: The Seasonal Cycle of Low Stratiform Clouds, *Journal of Climate*, 6, 1587-1606, 1993.

393 Klimont, Z., Smith, S. J., and Cofala, J.: The last decade of global anthropogenic sulfur dioxide: 2000-2011 emissions, *Environ Res Lett*, 8,
394 2013.

395 Lauer, A., Eyring, V., Hendricks, J., Jockel, P., and Lohmann, U.: Global model simulations of the impact of ocean-going ships on aerosols,
396 clouds, and the radiation budget, *Atmos Chem Phys*, 7, 5061-5079, 2007.

397 Lauer, A., Eyring, V., Corbett, J. J., Wang, C. F., and Winebrake, J. J.: Assessment of Near-Future Policy Instruments for Oceangoing
398 Shipping: Impact on Atmospheric Aerosol Burdens and the Earth's Radiation Budget, *Environ Sci Technol*, 43, 5592-5598, 2009.

399 Liu, X., Easter, R. C., Ghan, S. J., Zaveri, R., Rasch, P., Shi, X., Lamarque, J. F., Gettelman, A., Morrison, H., Vitt, F., Conley, A., Park, S.,
400 Neale, R., Hannay, C., Ekman, A. M. L., Hess, P., Mahowald, N., Collins, W., Iacono, M. J., Bretherton, C. S., Flanner, M. G., and
401 Mitchell, D.: Toward a minimal representation of aerosols in climate models: description and evaluation in the Community
402 Atmosphere Model CAM5, *Geosci Model Dev*, 5, 709-739, 2012.

403 Mahajan, A. S., Fadnavis, S., Thomas, M. A., Pozzoli, L., Gupta, S., Royer, S. J., Saiz-Lopez, A., and Simo, R.: Quantifying the impacts of an
404 updated global dimethyl sulfide climatology on cloud microphysics and aerosol radiative forcing, *J Geophys Res-Atmos*, 120, 2524-
405 2536, 2015.

406 Mahowald, N. M., Muhs, D. R., Levis, S., Rasch, P. J., Yoshioka, M., Zender, C. S., and Luo, C.: Change in atmospheric mineral aerosols in
407 response to climate: Last glacial period, preindustrial, modern, and doubled carbon dioxide climates, *J Geophys Res-Atmos*, 111,
408 2006.

409 Malavelle, F. F., Haywood, J. M., Jones, A., Gettelman, A., Clarisse, L., Bauduin, S., Allan, R. P., Karset, I. H. H., Kristjansson, J. E.,
410 Oreopoulos, L., Cho, N., Lee, D., Bellouin, N., Boucher, O., Grosvenor, D. P., Carslaw, K. S., Dhomse, S., Mann, G. W., Schmidt,
411 A., Coe, H., Hartley, M. E., Dalvi, M., Hill, A. A., Johnson, B. T., Johnson, C. E., Knight, J. R., O'Connor, F. M., Partridge, D. G.,
412 Stier, P., Myhre, G., Platnick, S., Stephens, G. L., Takahashi, H., and Thordarson, T.: Strong constraints on aerosol-cloud interactions
413 from volcanic eruptions, *Nature*, 546, 485-491, 10.1038/nature22974, 2017.

414 McCoy, D. T., Burrows, S. M. W., Robert, Grosvenor, D. P., Elliott, S. M., Ma, P.-L., Rasch, P. J., and Hartmann, D. L.: Natural aerosols
415 explain seasonal and spatial patterns of Southern Ocean cloud albedo, 1, 10.1126/sciadv.1500157, 2015.

416 Morrison, H., and Gettelman, A.: A new two-moment bulk stratiform cloud microphysics scheme in the community atmosphere model, version
417 3 (CAM3). Part I: Description and numerical tests, *Journal of Climate*, 21, 3642-3659, 2008.

418 Neubauer, D., Lohmann, U., Hoose, C., and Frontoso, M. G.: Impact of the representation of marine stratocumulus clouds on the anthropogenic
419 aerosol effect, *Atmos Chem Phys*, 14, 11997-12022, 2014.

420 Notteboom, T.: The impact of low sulphur fuel requirements in shipping on the competitiveness of ro-ro shipping in Northern Europe, *WMU*
421 *Journal of Maritime Affairs*, 10, 63-95, 10.1007/s13437-010-0001-7, 2010.

422 Pandis, S. N., Russell, L. M., and Seinfeld, J. H.: The Relationship between Dms Flux and Ccn Concentration in Remote Marine Regions, *J*
423 *Geophys Res-Atmos*, 99, 16945-16957, 1994.

424 Partanen, A. I., Laakso, A., Schmidt, A., Kokkola, H., Kuokkanen, T., Pietikainen, J. P., Kerminen, V. M., Lehtinen, K. E. J., Laakso, L., and
425 Korhonen, H.: Climate and air quality trade-offs in altering ship fuel sulfur content, *Atmos Chem Phys*, 13, 12059-12071, 2013.

426 Peters, K., Stier, P., Quaas, J., and Grassl, H.: Aerosol indirect effects from shipping emissions: sensitivity studies with the global aerosol-
427 climate model ECHAM-HAM, *Atmos Chem Phys*, 12, 5985-6007, 2012.

428 Peters, K., Stier, P., Quaas, J., and Grassl, H.: Corrigendum to "Aerosol indirect effects from shipping emissions: sensitivity studies with the
429 global aerosol-climate model ECHAM-HAM" published in *Atmos. Chem. Phys.*, 12, 5985-6007, 2012, *Atmos Chem Phys*, 13,
430 6429-6430, 10.5194/acp-13-6429-2013, 2013.

431 Peters, K., Quaas, J., Stier, P., and Graßl, H.: Processes limiting the emergence of detectable aerosol indirect effects on tropical warm clouds in
432 global aerosol-climate model and satellite data, *Tellus B: Chemical and Physical Meteorology*, 66, 24054,
433 10.3402/tellusb.v66.24054, 2014.

434 Possner, A., Zubler, E., Lohmann, U., and Schär, C.: The resolution dependence of cloud effects and ship-induced aerosol-cloud interactions in
435 marine stratocumulus, *Journal of Geophysical Research: Atmospheres*, 121, 4810-4829, 10.1002/2015jd024685, 2016.

436 Pringle, K. J., Tost, H., Pozzer, A., Pöschl, U., and Lelieveld, J.: Global distribution of the effective aerosol hygroscopicity parameter for CCN
437 activation, *Atmos Chem Phys*, 10, 5241-5255, 10.5194/acp-10-5241-2010, 2010.

438 Quinn, P. K., Bates, T. S., Covert, D. S., Ramsey-Bell, D. C., and McInnes, L.: Dimethylsulphide: Oceans, Atmosphere and Climate, in: *Air*
439 *Pollution Research Reports*, 1 ed., edited by: Restelli, G., and Angeletti, G., 43, Springer Netherlands, 400, 1993.

440 Righi, M., Klinger, C., Eyring, V., Hendricks, J., Lauer, A., and Petzold, A.: Climate Impact of Biofuels in Shipping: Global Model Studies of
441 the Aerosol Indirect Effect, *Environ Sci Technol*, 45, 3519-3525, 2011.

442 Rothenberg, D., and Wang, C.: Metamodeling of Droplet Activation for Global Climate Models, *J Atmos Sci*, 73, 1255-1272, 2016.

443 Rothenberg, D., and Wang, C.: An aerosol activation metamodel of v1.2.0 of the pyrcl cloud parcel model: development and offline
444 assessment for use in an aerosol-climate model, *Geosci Model Dev*, 10, 1817-1833, 2017.

445 Rothenberg, D., Avramov, A., and Wang, C.: On the representation of aerosol activation and its influence on model-derived estimates of the
446 aerosol indirect effect, *Atmos Chem Phys*, 18, 7961-7983, 10.5194/acp-18-7961-2018, 2018.

447 Russell, L. M., Pandis, S. N., and Seinfeld, J. H.: Aerosol Production and Growth in the Marine Boundary-Layer, *J Geophys Res-Atmos*, 99,
448 20989-21003, 1994.

449 Scanza, R. A., Mahowald, N., Ghan, S., Zender, C. S., Kok, J. F., Liu, X., Zhang, Y., and Albani, S.: Modeling dust as component minerals in
450 the Community Atmosphere Model: development of framework and impact on radiative forcing, *Atmos Chem Phys*, 15, 537-561,
451 2015.

452 Schreier, M., Mannstein, H., Eyring, V., and Bovensmann, H.: Global ship track distribution and radiative forcing from 1 year of AATSR data,
453 *Geophys Res Lett*, 34, 2007.

454 Tesdal, J. E., Christian, J. R., Monahan, A. H., and von Salzen, K.: Sensitivity of modelled sulfate aerosol and its radiative effect on climate to
455 ocean DMS concentration and air-sea flux, *Atmos Chem Phys*, 16, 10847-10864, 2016.

456 Thomas, M. A., Suntharalingam, P., Pozzoli, L., Rast, S., Devasthale, A., Kloster, S., Feichter, J., and Lenton, T. M.: Quantification of DMS
457 aerosol-cloud-climate interactions using the ECHAM5-HAMMOZ model in a current climate scenario, *Atmos Chem Phys*, 10, 7425-
458 7438, 2010.

459 Thomas, M. A., Suntharalingam, P., Pozzoli, L., Devasthale, A., Kloster, S., Rast, S., Feichter, J., and Lenton, T. M.: Rate of non-linearity in
460 DMS aerosol-cloud-climate interactions, *Atmos Chem Phys*, 11, 11175-11183, 2011.

461 Warren, S. G., Hahn, C. J., London, J., Chervin, R. M., and Jenne, R. L.: Global Distribution of Total Cloud Cover and Cloud Type Amounts
462 Over Ocean, NCAR Technical Note NCAR/TN-273+STR, doi:10.5065/D6GH9FXB, 1988.

463 Winebrake, J. J., Corbett, J. J., Green, E. H., Lauer, A., and Eyring, V.: Mitigating the Health Impacts of Pollution from Oceangoing Shipping:
464 An Assessment of Low-Sulfur Fuel Mandates, *Environ Sci Technol*, 43, 4776-4782, 2009.

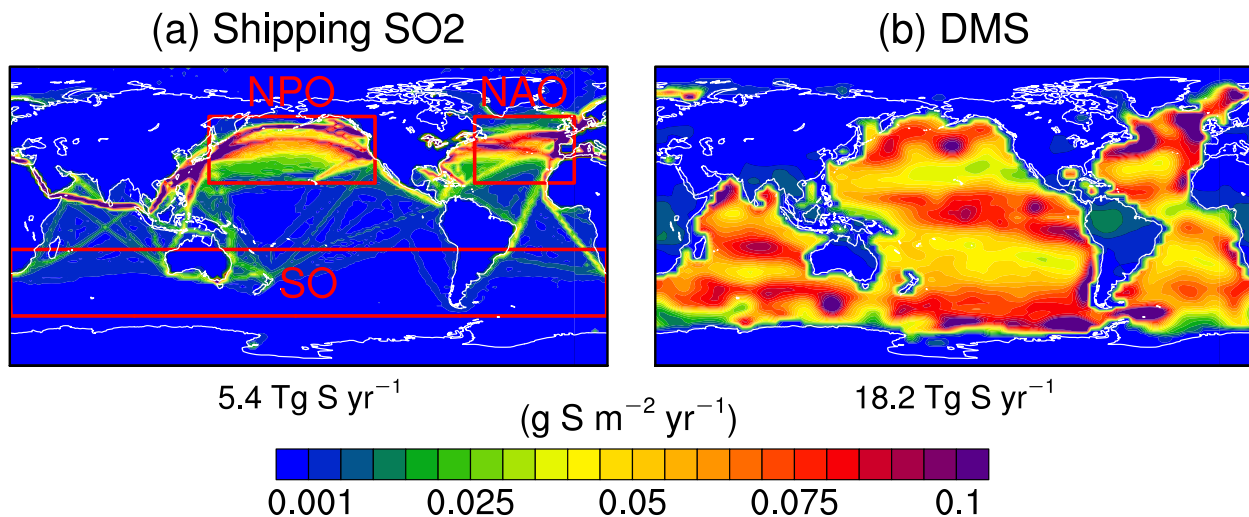
465

466 **Table 1. Summary of experiments.**

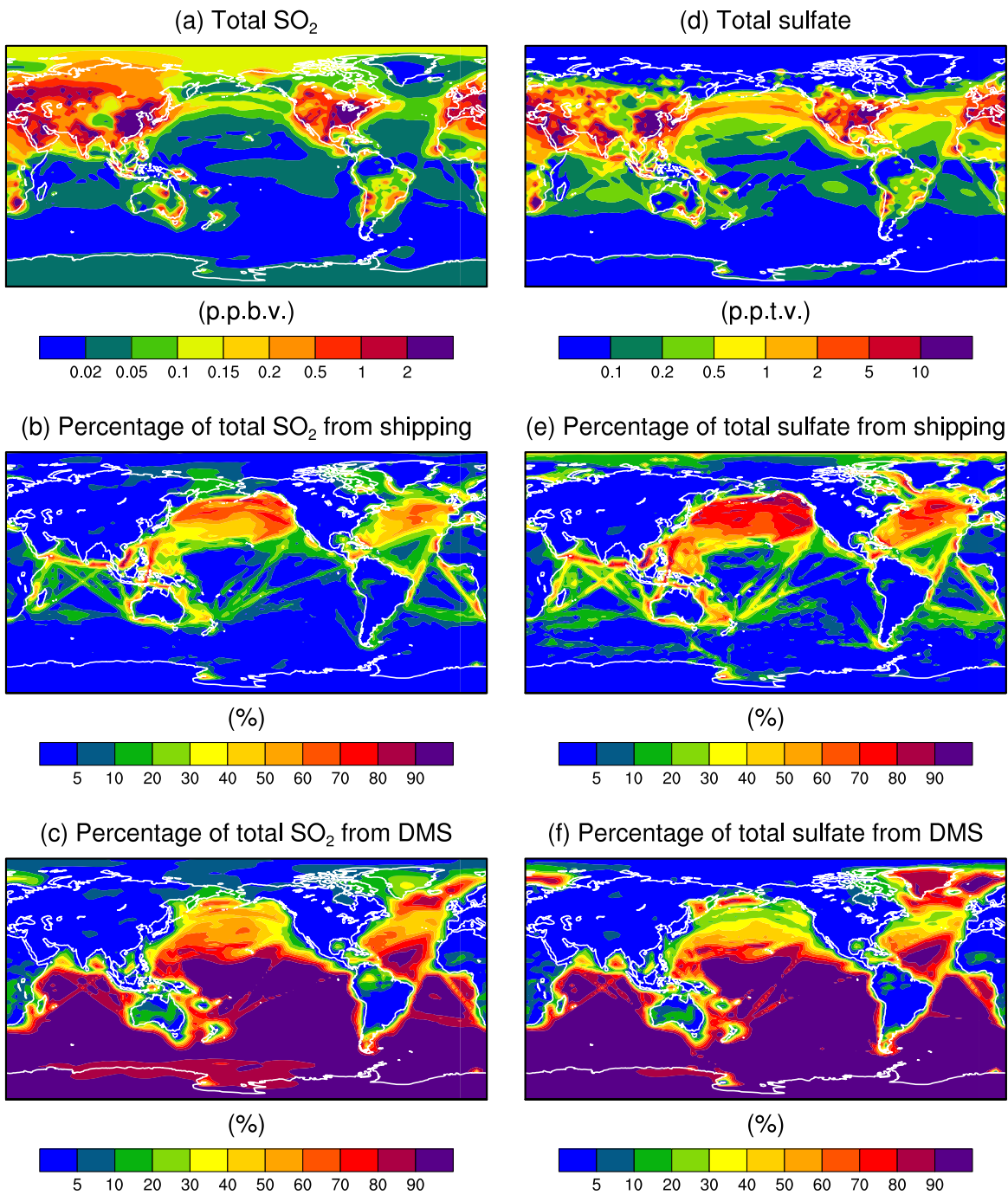
Aerosol Modules	Experiments	DMS emissions	Ship emissions	Description
MARC	Shipping	<i>DMSRef</i>	<i>ShipZero</i>	DMS emission (Tg S yr ⁻¹): DMSZero: 0 DMSLow: 9.1 DMSRef: 18.2 Ship emission (Tg S yr ⁻¹): ShipZero: 0 ShipLow: 1.0 (0.5%) ShipRef: 5.4 (2.7%) ShipHigh: 7.0 (3.5%)
			<i>ShipLow</i>	
			<i>ShipRef</i>	
			<i>ShipHigh</i>	
	DMS	<i>DMSZero</i>	<i>ShipZero</i>	
			<i>ShipRef</i>	
<i>DMSLow</i>	<i>ShipZero</i>			
	<i>ShipRef</i>			
MAM3	DMS	<i>DMSRef</i>	<i>ShipZero</i>	
			<i>ShipRef</i>	
		<i>DMSZero</i>	<i>ShipZero</i>	
			<i>ShipRef</i>	
		<i>DMSLow</i>	<i>ShipZero</i>	
			<i>ShipRef</i>	

467 Notes: in *ShipZero* experiments, emission rates of all gas-phase and aerosol species from shipping emissions are set to zero; while
 468 in *ShipLow*, *ShipRef*, and *ShipHigh* experiments, all shipping emission rates (such as OC and BC) are set to [observationsyear-2000](#)
 469 [values](#) except for emission rates of sulfur compounds (i.e. SO₂ and SO₄) which are modified. [The percent for ship emission in the](#)
 470 [last column stands for the proportion of sulfur content in the heavy fuel oils by mass.](#)

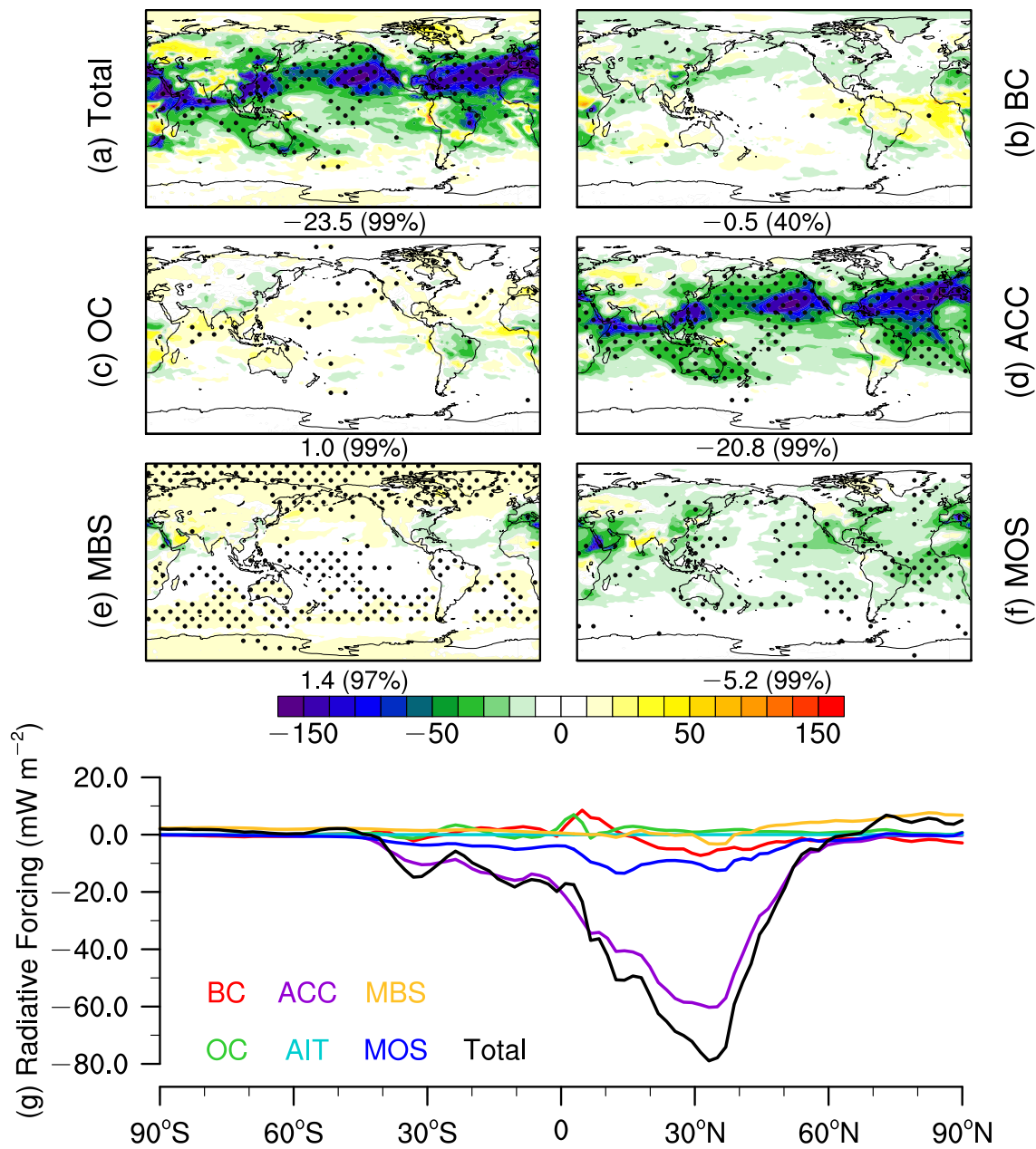
471



472 **Figure 1. Spatial patterns of annual means of sulfur emission (g S m⁻² yr⁻¹) from (a) international shipping and (b) natural DMS in the**
 473 **simulation at the reference emission level (i.e., *ShipRef*/*DMSRef*).** The numbers below each panel are the global total annual emissions.
 474 **Three regions are selected for further analysis: The North Pacific Ocean (NPO; 20°N–60°N, 140°E–240°E), the North Atlantic Ocean**
 475 **(NAO; 20°N–60°N, 300°E–360°E), and the Southern Ocean (SO; 20°S–60°S, 0°E–360°E).**
 476



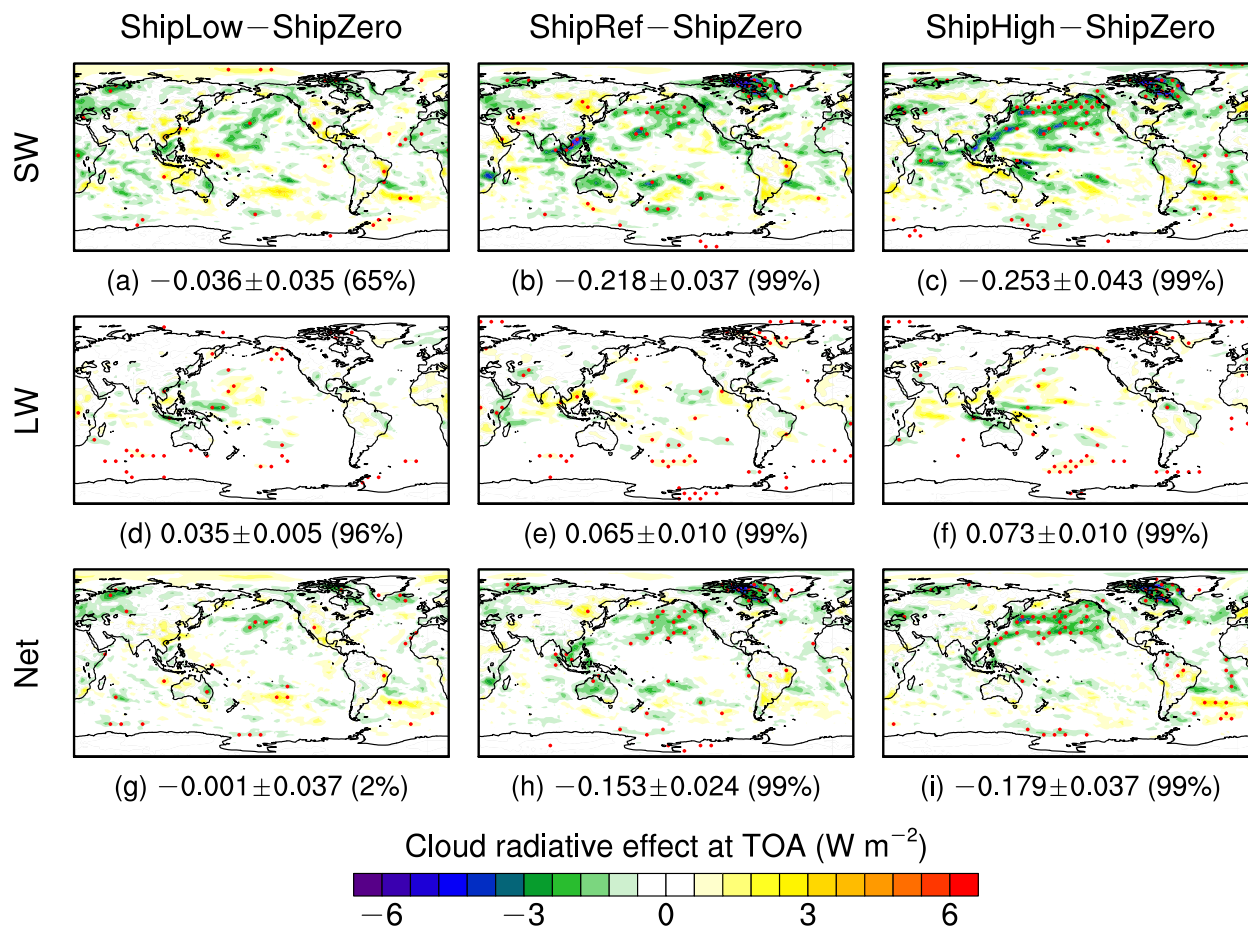
477
 478 **Figure 2.** Spatial patterns of (a) annual mean concentrations of total SO₂ (units: parts per billion by volume; ppbv), (b) and (c) are
 479 respectively the contributions of shipping emission and natural DMS to total SO₂ in the lowest model layer. (d)–(f) are the same as (a)–
 480 (c), but for sulfate aerosols. These results are from MARC simulations and calculated as the differences between the simulations with
 481 the international shipping and DMS emissions at the reference and zero levels (i.e., *ShipRef_DMSRef* minus *ShipZero_DMSRef* and
 482 *ShipRef_DMSRef* minus *ShipRef_DMSZero*).



483

484 Figure 3. Simulated direct radiative effect (DRE; units: mW m^{-2}) of ISE at TOA by MARC. The DRE is calculated as the difference
 485 between simulation results with and without ISE (i.e., *ShipRef_DMSRef* minus *ShipZero_DMSRef*) and averaged over the 30-year period
 486 of simulations at all-sky conditions. Panels (a)–(f) show the spatial patterns of DRE due to ISE with the global mean differences and the
 487 associated significant levels indicated by the numbers below each panel and panel (g) is the meridional variations of zonal mean DRE
 488 for various aerosol types from ISE and their total effects. The expansions of the abbreviations can be found in Section 2.3. The black
 489 dots represent grid points that are statistically significant above the 90% confidence level based on the two-tailed Student's *t*-test.

DMSRef



490

491 **Figure 4.** Spatial patterns of MARC simulated cloud radiative effect (CRE; units: W m^{-2}) at TOA of ISE with various shipping emission
 492 levels. The CRE is calculated as the differences of radiation flux at TOA and at all-sky conditions between the simulation without shipping
 493 emissions and three simulations with the same DMS emissions at the reference level but various shipping emission levels (i.e., low,
 494 reference, high) in short-wave (SW), long-wave (LW), and net (SW+LW) and averaged over the 30-year simulation period. The numbers
 495 below each panel are the global means, standard deviation across the 30-year period, and the confidence level. The red dots represent
 496 grid points that are statistically significant above the 90% confidence level based on the two-tailed Student's *t*-test.

497

498

499

500

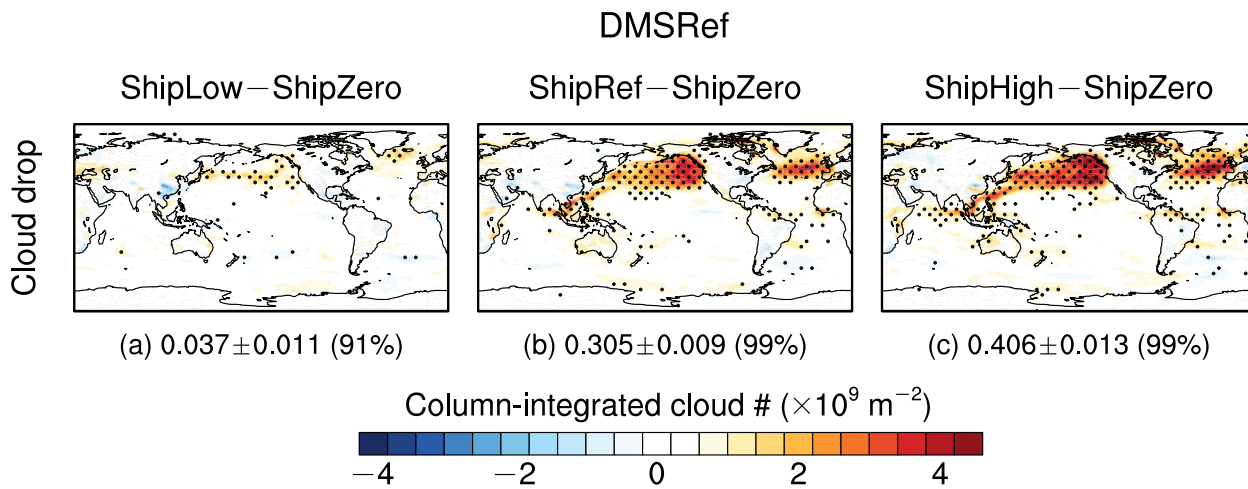
501

502

503

504

505



506

507 **Figure 5. Spatial patterns of MARC simulated column-integrated cloud droplet number concentration ($\times 10^9 \text{ m}^{-2}$) response to**
 508 **international shipping emissions. The responses are calculated as the differences of cloud droplet number integrated through the whole**
 509 **atmospheric columns between the simulation without shipping emissions and three simulations with the reference shipping emission and**
 510 **various DMS emissions (i.e., zero, low, and reference) over the 30-year simulation period. The numbers below each panel are the global**
 511 **means, standard deviation across the 30-year period, and the confidence level. The black dots represent grid points that are statistically**
 512 **significant above the 90% confidence level based on the two-tailed Student's *t*-test.**

513

514

515

516

517

518

519

520

521

522

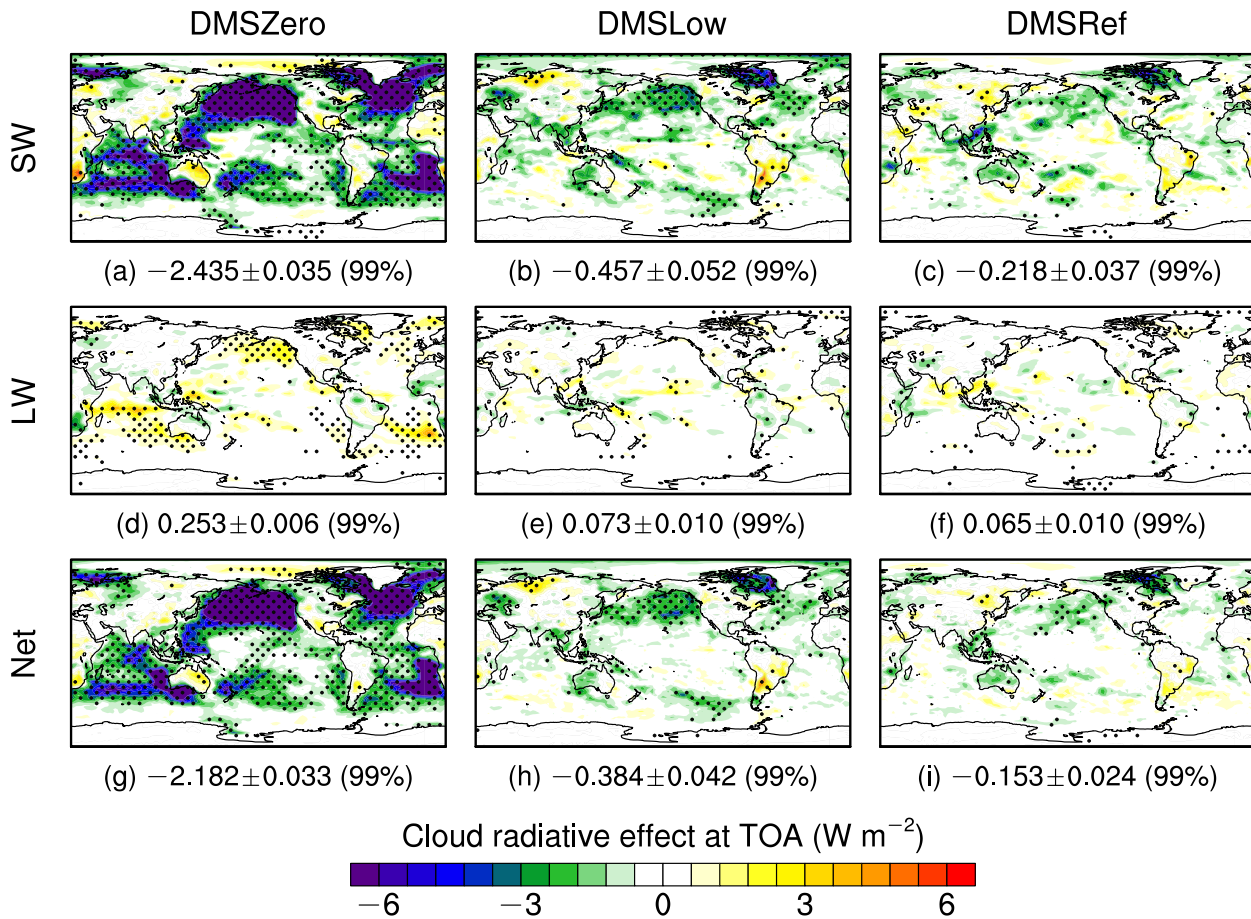
523

524

525

526

ShipRef – ShipZero



527

528 **Figure 6. Spatial patterns of MARC simulated cloud radiative effect (CRE; units: W m^{-2}) at TOA of ISE at various DMS emission levels.**
 529 **The CRE is calculated as the differences of radiation flux at TOA and at all-sky conditions between the simulation without shipping**
 530 **emissions and three simulations with the same shipping emissions at the reference level but various DMS emission levels (i.e., zero, low,**
 531 **and reference) in short-wave (SW), long-wave (LW), and net (SW+LW) and averaged over the 30-year simulation period. The numbers**
 532 **below each panel are the global means, standard deviation across the 30-year period, and the confidence level. The black dots represent**
 533 **grid points that are statistically significant above the 90% confidence level based on the two-tailed Student's *t*-test.**

534

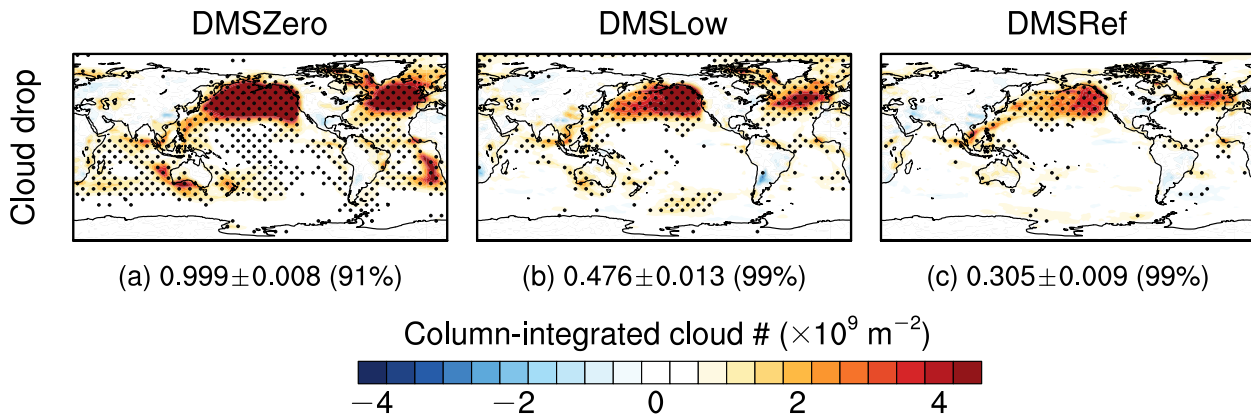
535

536

537

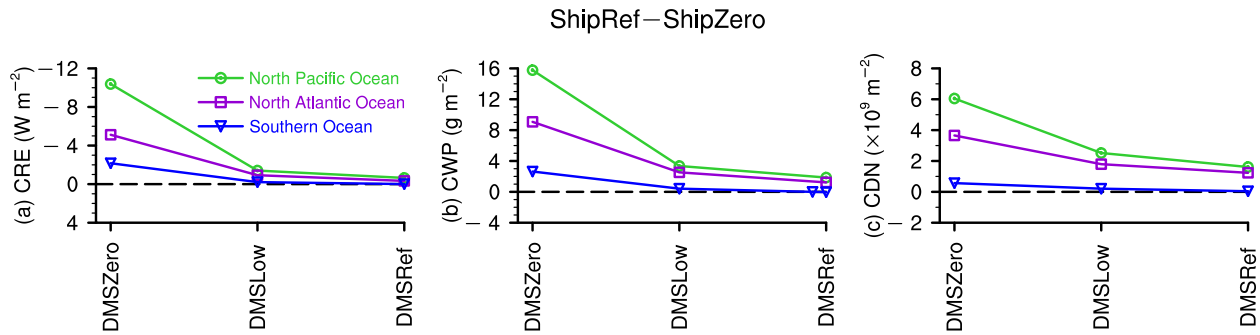
538

ShipRef – ShipZero



539

540 **Figure 7. Spatial patterns of MARC simulated column-integrated cloud droplet number concentration ($\times 10^9 \text{ m}^{-2}$) response to**
 541 **international shipping emissions. The responses are calculated as the differences of cloud droplet number integrated through the whole**
 542 **atmospheric columns between the simulation without shipping emissions and three simulations with the reference shipping emission and**
 543 **various DMS emissions (i.e., zero, low, and reference) over the 30-year simulation period. The numbers below each panel are the global**
 544 **means, standard deviation across the 30-year period, and the confidence level. The black dots represent grid points that are statistically**
 545 **significant above the 90% confidence level based on the two-tailed Student's *t*-test.**



546

547 **Figure 8. Impacts of DMS emissions on cloud responses to international shipping emissions. (a) Cloud radiative effects at TOA (W m^{-2}),**
 548 **(b) column-integrated cloud water path (g m^{-2}), and (c) column-integrated cloud droplet number ($\times 10^9 \text{ m}^{-2}$). The green, purple, and blue**
 549 **curves respectively represent quantities area-averaged over the North Pacific Ocean (NPO), the North Atlantic Ocean (NAO), and the**
 550 **Southern Ocean (SO), which are shown as red boxes in Figure 1a. These results are from MARC simulations.**

551

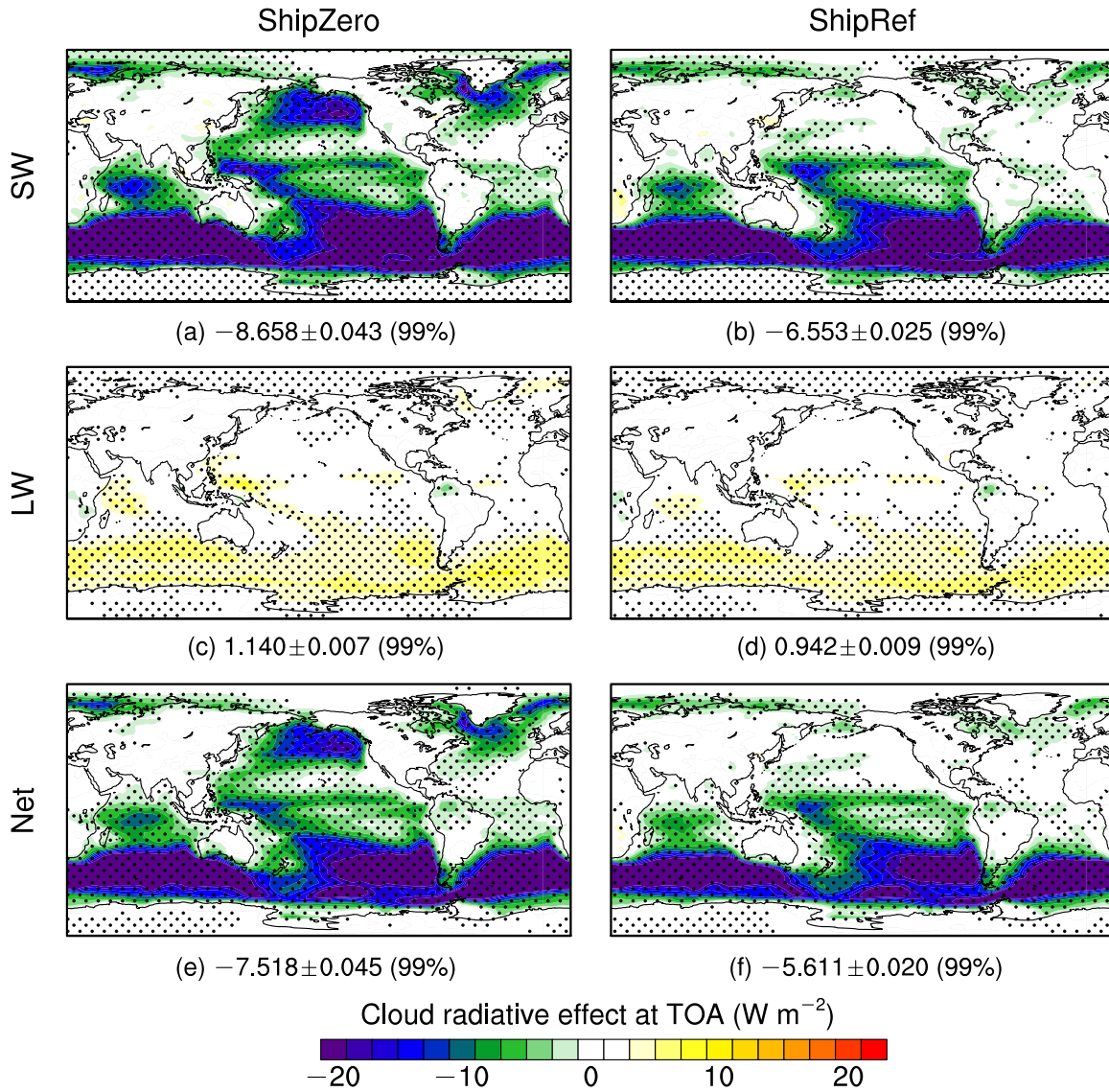
552

553

554

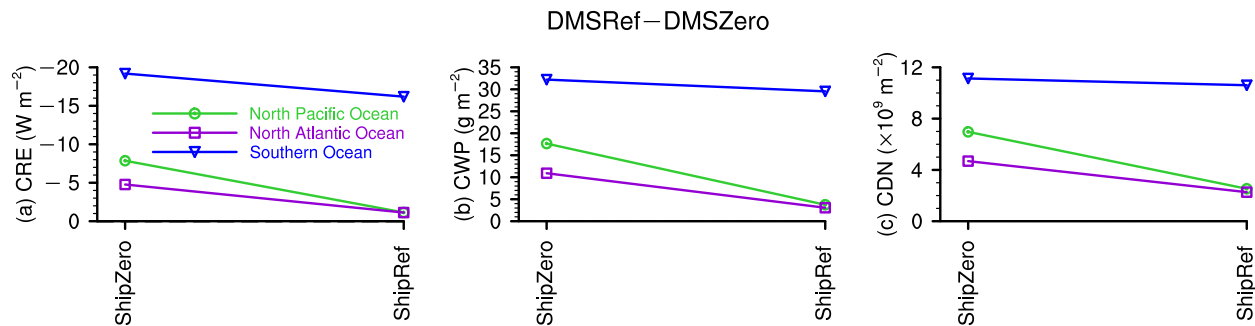
555

DMSRef – DMSZero



556

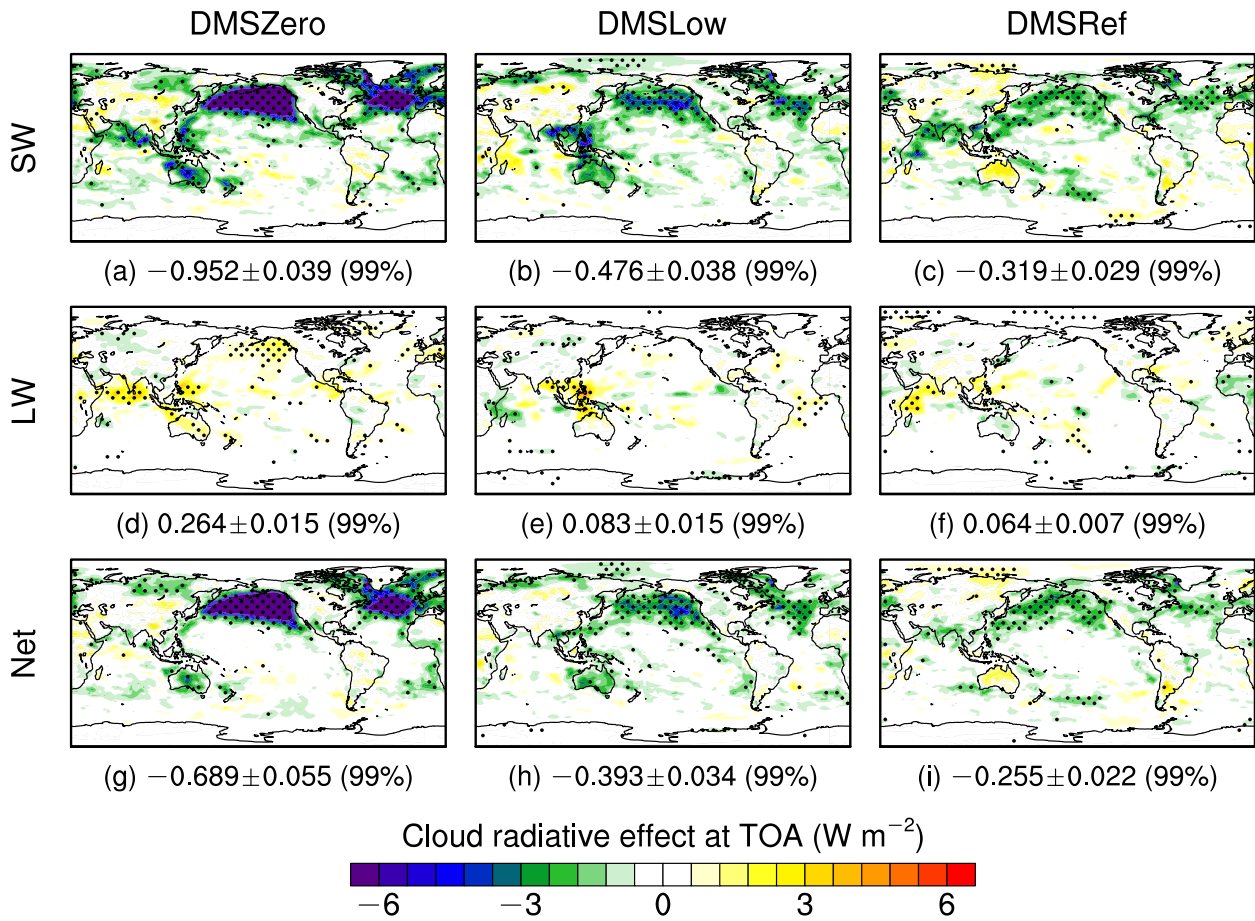
557 **Figure 9.** Spatial patterns of MARC simulated cloud radiative effect (units: $W m^{-2}$) of DMS emissions at various shipping emission levels.
 558 The CRE is calculated as the differences of radiation flux at TOA and at all-sky conditions between the simulation without DMS
 559 emissions and two simulations with the same DMS emissions at the reference level but various shipping emission levels (i.e., zero and
 560 reference) in short-wave (SW), long-wave (LW), and net (SW+LW) and averaged over the 30-year simulation period. The numbers
 561 below each panel are the global means, standard deviation across the 30-year period, and the confidence level. The black dots represent
 562 grid points that are statistically significant above the 90% confidence level based on the two-tailed Student's t -test.



563

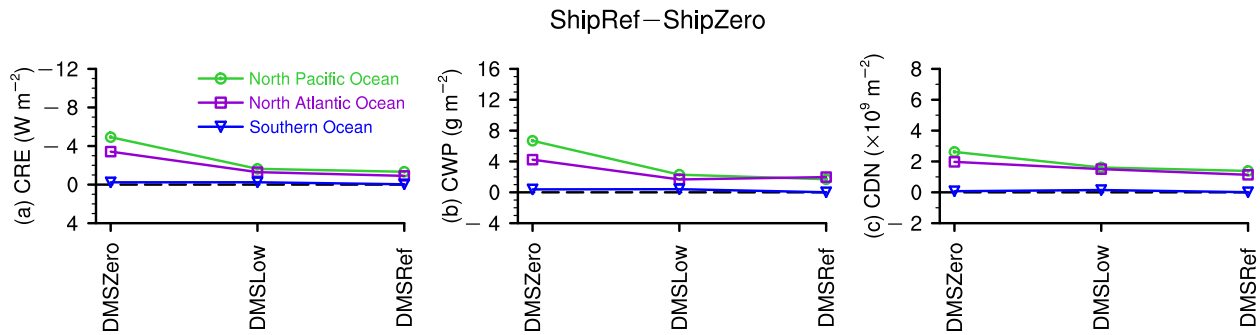
564 **Figure 10.** Impacts of ISE on cloud responses to DMS emissions. (a) Cloud radiative effects at TOA ($W m^{-2}$), (b) column-integrated cloud
 565 water path ($g m^{-2}$), and (c) column-integrated cloud droplet number ($\times 10^9 m^{-2}$). The green, purple, and blue curves respectively represent
 566 quantities area-averaged over the North Pacific Ocean (NPO), the North Atlantic Ocean (NAO), and the Southern Ocean (SO), which
 567 are shown as red boxes in Figure 1a. These results are from MARC simulations.

ShipRef – ShipZero



568

569 Figure 11. Same as Figure 6, but using a different aerosol module, namely MAM3 rather than MARC.



570

571 Figure 12. Same as Figure 8, but using a different aerosol module, namely MAM3 rather than MARC.